creative commons
COMMONS DEED

저작자표시-비영리-변경금지 2.0 대한민국

이용자는 아래의 조건을 따르는 경우에 한하여 자유롭게

- 이 저작물을 복제, 배포, 전송, 전시, 공연 및 방송할 수 있습니다.

다음과 같은 조건을 따라야 합니다:

**저작자표시**. 귀하는 원저작자를 표시하여야 합니다.

**비영리**. 귀하는 이 저작물을 영리 목적으로 이용할 수 없습니다.

**변경금지**. 귀하는 이 저작물을 개작, 변형 또는 가공할 수 없습니다.

- 귀하는, 이 저작물의 재이용이나 배포의 경우, 이 저작물에 적용된 이용허락조건을 명확하게 나타내어야 합니다.
- 저작권자로부터 별도의 허가를 받으면 이러한 조건들은 적용되지 않습니다.

**저작권법에 따른 이용자의 권리는 위의 내용에 의하여 영향을 받지 않습니다.**

이것은 이용허락규약(Legal Code)을 이해하기 쉽게 요약한 것입니다.

Disclaimer

dCollection

의학박사 학위논문

# 생체막 모방 고분자 코팅을 시행한 고어텍스의 항염 항균 작용 상승 효과

# Anti-inflammatory and anti-bacterial effect of covalently attached biomembrane-mimic polymer grafts on Gore-Tex implants

2017 년 8 월

서울대학교 대학원

임상의과학과

진 영 주

# ABSTRACT

## Anti-inflammatory and anti-bacterial effect of covalently attached biomembrane-mimic polymer grafts on Gore-Tex implants

Young Ju Jin

Department of Clinical Medical Sciences

The Graduate School

Seoul National University

**Introduction**: Expanded polytetrafluoroethylene (ePTFE), also known as Gore-Tex, is widely used as an implantable biomaterial in biomedical applications owing to its favorable mechanical properties and biochemical inertness. However, infection and inflammation are two major complications with ePTFE implantations. To minimize these complications, i covalently grafted a biomembrane-mimic polymer, poly(2-methacryloyloxylethyl phosphorylcholine) (PMPC), by partial defluorination followed by UV-induced polymerization with cross-linkers on the ePTFE surface. The aim of this study is to evaluate the effects of PMPC grafting on ePTFE.

**Methods:** Water contact angle, X-ray photoelectron spectroscopy, scanning electron microscopy and universal test machine analysis were measured to evaluate surface modification of PMPC grafted ePTFE plates. In vitro, for the evaluation of anti-inflammatory response, protein adsorption, fibroblast adhesion and bacterial attachment test were performed. In vivo, thirty-four female Sprague-Dawley rats were implanted with both non-grafted ePTFE and PMPC grafted ePTFE plates on the each side of back. At each time point of 24 hour and 72 hour, 8 rats were sacrificed and at 4 and 12 weeks, 9 rats were sacrificed respectively.

**Results:** PMPC grafting greatly reduced serum protein adsorption as well as fibroblast adhesion on the ePTFE surface. Moreover, the PMPC-grafted ePTFE surface exhibited a dramatic inhibition of the adhesion and growth of *Staphylococcus aureus*, a typical pathogenic bacterium in ePTFE implantation, in the porous network. Based on an analysis of immune cells and inflammation-related factors, i.e. transforming growth factor-β (TGF-β) and myeloperoxidase (MPO) were significantly reduced in PMPC grafted ePTFE compare to non-grafted ePTFE.

**Conclusions**: I confirmed that inflammation was efficiently alleviated in tissues around PMPC-grafted ePTFE plates implanted in the backs of rats. Covalent PMPC may be an effective strategy to promote anti-inflammatory and anti-bacterial functions in ePTFE implants and to reduce side effects in biomedical applications of ePTFE.

**Keywords :** expanded polytetrafluoroethylene (ePTFE), biomembrane-mimic polymer, poly(2-methacryloyloxylethyl phosphorylcholine) (PMPC), infection, grafting, inflammation

**Student number:** 2014-30921

# CONTENTS

# LIST OF TABLES AND FIGURES

# LIST OF ABBREVIATIONS

ePTFE : Expanded polytetrafluoroethylene

PMPC : Poly(2-methacryloyloxylethyl phosphorylcholine)

XPS : X-ray photoelectron spectroscopy

SEM : Scanning electron microscopy

IHC : Immunohistochemistry

TGF-β : Transforming growth factor-β

MPO : Myeloperoxidase

# Introduction

Polytetrafluoroethylene (PTFE) is widely used in various fields owing to its inertness and abnormally low surface energy.[1] Among various materials-based on PTFE, expanded polytetrafluoroethylene (ePTFE), commonly known as Gore-Tex, has been increasingly used in the textile industry because of its waterproof property and vapor-selective permeability, which is attributed to its micrometer-sized pore structure.[2] Moreover, biochemical inertness, mechanical strength, and relatively easy formability of ePTFE are attractive characteristics for biomaterials; accordingly it is commonly used as a platform for artificial heart valves and vessels,[3] fistulas for hemodialysis,[4] artificial ligaments,[5] and implants for reconstructive or plastic surgery.[6]

Although the chemically and biologically inert surface of ePTFE is generally considered highly biocompatible, serious complications have been reported in biomedical applications. More seriously, ePTFE with a pore sizes of 10–30 μm potentially provides an ideal habitat for pathogenic bacteria because it is difficult for eukaryotic immune cells to penetrate the porous structure.[2] Therefore, infection and inflammation occur in up to 3.7% of recipients after ePTFE implantation.[2,6] Excessive inflammation could also be induced, irrespective of pathogenic bacterial infection. The fluorocarbon surface of ePTFE could partially inhibit the non-specific adsorption of biomolecules, but significant amounts of albumin, immunoglobulin, fibrinogen, or proteoglycans can be adsorbed on the surface in physiological fluids.[7] The denatured

conformation of adsorbed proteins on hydrophobic surfaces is recognized by the host immune system, provoking excessive foreign body reactions including inflammation, fibrosis, and even tissue necrosis.[2,8-10] Furthermore, thrombosis caused by platelet adhesion on the ePTFE surface is one of the most catastrophic complications with ePTFE-based heart valves and vessels implantation.[11,12] Antibiotics, anti-inflammatory, and immunosuppressant drugs or anti-thrombotic drugs could alleviate these complications temporarily,[13] but we predicted that the surface modification of ePTFE by covalent grafting is a semi-permanent solution to reduce complications, considering that excessive foreign body reactions often occur for many years.[14,15]

Zwitterionic polymers show effective anti-fouling effects in various applications.[16-18] Zwitterionic functional groups with neighboring positively and negatively charged groups form thick hydration shells and inhibit non-specific interactions with other hydrophobic or hydrophilic molecules in aqueous solutions.[16-18] A representative biocompatible zwitterionic polymer is 2-methacryloryloxyethyl phosphorylcholine (MPC)-based polymer.[19] MPC-based polymers possess phosphorylcholine side chains mimicking the head group of phosphatidylcholine in the eukaryotic membrane. The polymers exhibit outstanding anti-protein-adsorption activity in physiological fluids and are used as a coating material for coronary stents[20,21] and artificial vessels[22] with hemocompatibility and anti-thrombotic activity, artificial joints with anti-osteolytic activity,[23] and silicone implants with anti-fibrotic activity.[24] MPC-based coatings can also inhibit bacterial adhesion on hydroxyapatite in the oral

cavity.[25] In addition, it was reported that porous polyethylene-based substrates coated with MPC-based polymers exhibited low inflammatory responses around the tissues.[26] Therefore, i expected that the most serious complications of ePTFE implants, inflammation and infection, might be overcome in a semi-permanent manner by the covalent grafting of poly(2-methacryloryloxyethyl phosphorylcholine) (PMPC) on ePTFE surfaces. However, the covalent grafting of polymers on the ePTFE surface is difficult owing to the chemical inertness of its carbon-fluorine bonds.[27]

In this study, i developed an efficient method for polymer grafting on ePTFE implants using partial reduction and UV-induced polymerization with appropriate cross-linkers (Figure1). Efficient PMPC grafting on the ePTFE surface was confirmed by analyses of the water contact angle, X-ray photoelectron spectroscopy (XPS), and Fourier transform infrared spectroscopy (FT-IR). After i confirmed that the microstructure and mechanical properties of ePTFE were not affected by grafting, i compared the adsorption of proteins and the adhesion and growth of fibroblasts and *Staphylococcus aureus*, a representative pathogenic bacterium that causes serious infection in ePTFE implantation,[28,29] on non-grafted and grafted surfaces. Finally, i subcutaneously implanted the PMPC-grafted ePTFE plates into the backs of rats, and observed the effects on inflammation by evaluating inflammatory cells and important inflammation-related factors, such as transforming growth factor-β (TGF-β) and myeloperoxidase (MPO), in neighboring tissues around the ePTFE implants.

*in vivo* analysis of PMPC-grafted ePTFE implants improves my understanding of foreign body reactions and inflammation around the implants. The biomedical applications of ePTFE could be extended by combining the attractive properties of ePTFE with the anti-inflammatory and anti-bacterial properties of PMPC grafts. Surface grafting could be an effective strategy for the preparation of an ideal implantable material in clinical applications.

# Materials and methods

## Materials

2-Methacryloyloxyethyl phosphorylcholine (MPC) monomers were purchased from KCI (Korea). Benzophenone (BP), sodium hydride (NaH), anhydrous *N*,*N*-dimethylformamide (DMF), dipentaerythritol penta-/hexa-acrylate, ethylene glycol dimethacrylate, bovine serum albumin (BSA), bovine plasma fibrinogen (BPF), protease inhibitor cocktail (PIC), and Tween-20 were purchased from Sigma-Aldrich (St. Louis, MO, USA). Acetone, ethanol, and dichloromethane were purchased from Daejung (Busan, Korea). Dulbecco's phosphate-buffered saline (DPBS, without calcium chloride and magnesium chloride), Dulbecco's modified Eagle's medium (DMEM) and fetal bovine serum (FBS) were purchased from WelGENE (USA). Brain heart infusion broth was purchased from MB Cell (Korea). A Micro-BCA Protein Assay Reagent Kit was purchased from Pierce Chemical (Rockford, IL, USA). The Cell Counting Kit-8 (CCK-8) was purchased from Dojindo (Rockville, MD, USA). The enzyme-linked immunosorbent assay (ELISA) kits were purchased from MyBioSource (USA). The ePTFE (Gore-Tex) patch (Cat. No. 1310015020) was purchased from W.L. Gore & Associates (Wall Township, NJ, USA) and PTFE plates were purchased from Kyungshin (Incheon, Korea). Multiplex cytokine analysis kits (Cat. No. LMSAHM) were obtained from R&D Systems (USA).

**Surface reduction of ePTFE plates**

The ePTFE patch was cut into a square-shaped plate (1.5 cm × 1.5 cm × 2.0 mm). The ePTFE plate was washed with acetone and sonicated in deionized water to clean the surface. The surface of the ePTFE plate was partially reduced according to a previously described method.[30] BP (0.86 g) and NaH (0.40 g) were dissolved in anhydrous DMF (50 mL). The ePTFE plates were immersed in DMF solution and UV-irradiated (8 mW/cm$^2$, $\lambda_{max}$ = 365 nm) with a 100 W high-pressure mercury lamp (Lichtzen, Korea) for 20 min at 40℃. After irradiation, the ePTFE plate was thoroughly washed with DMF, dichloromethane, and distilled water, successively. The washed plates were dried in a vacuum oven overnight at 50℃. The surfaces of unexpanded PTFE plates were reduced following the same methods.

**PMPC grafting on ePTFE plates**

The surface-reduced ePTFE plates were covalently coated with PMPC according to previously described methods with modifications.[24] Briefly, the surface-reduced ePTFE plates were immersed in an initiator solution composed of BP (55 mM) as a photoinitiator and dipentaerythritol penta-/hexa-acrylate (2.5 mM) as a cross-linker in acetone. After immersion for 1 min, the ePTFE plates were dried in a vacuum for 1 h. The dried plates were immersed in an aqueous solution of MPC monomers (0.50 M) and a cross-linker (ethylene glycol dimethacrylate, 5.0 mM), and UV irradiated (1.2 W/cm$^2$, $\lambda_{ma}$ = 385 nm) for 20 min by a 600 W high-pressure mercury lamp (MS UV, Korea) at 25℃. After UV-initiated polymerization, the coated ePTFE plates were thoroughly

rinsed with acetone, water, and 70% (v/v) ethanol in water. After lyophilization, the plates were stored in 70% ethanol until use. The surface-reduced PTFE plates were grafted with PMPC following the same methods.

**Measurement of water contact angle**

The dynamic water contact angles were measured using a goniometer (Korea). The advancing contact angle was measured as the water volume was increased from 0 to 6 μL, and the receding contact angle was measured as the water volume was decreased from 6 to 3 μL.

**X-ray photoelectron spectroscopy**

A surface elemental analysis of ePTFE plates was conducted using XPS (AXIS-HIS; Kratos-Shimadzu, Kyoto, Japan) with Mg $K_\alpha$ (15 kV) in Mg/Al dual anode sources. The X-ray detector was 45° from the surface of the sample.

**Fourier transform infrared spectroscopy analysis**

The functional group vibrations of non-grafted and PMPC-grafted ePTFE were analyzed by FT-IR spectroscopy. The FT-IR spectra were examined in 32 scans over the range of 650–4000 $cm^{-1}$ at a resolution of 8.0 $cm^{-1}$ using an FT-IR instrument (Nicolet 6700; Thermo Scientific, Waltham, MA, USA).

**Scanning electron microscopy**

The surface morphology of ePTFE plates was observed by scanning electron microscopy (SEM; Hitachi S-4300, Tokyo, Japan). Samples were sputtered

with Pt and observed by microscopy. The surfaces of four plates were analyzed by SEM for each coating condition. Nine SEM images were analyzed to measure the pore size of the ePTFE and the thickness of the PMPC layer for each plate.

**Universal test machine (UTM) analysis**

The mechanical strengths of non-grafted and PMPC-grafted ePTFE plates were compared using a universal test machine (UTM; Quasar 5, Italy) with a 5 kN load cell. Each sample (20 × 0.5 × 2 mm) was measured at a preload value of 0.700 N and a test speed of 50.0 mm/min.

**Protein adsorption test**

Non-grafted and PMPC-grafted PTFE plates were incubated with mild shaking in a BSA (4.5 mg/mL) solution or in a BPF (0.3 mg/mL) solution. After a 1-h incubation period at 37℃, the plates were washed with DPBS twice. The amount of adsorbed protein was evaluated using the BCA Protein Assay Kit. Absorbance at a wavelength of 562 nm was measured using a spectrophotometric microplate reader (V-650; Jasco, Germany).

**Eukaryotic cell adhesion test**

The ePTFE plates were placed in a 24-well plate and mouse fibroblast cells (NIH-3T3) were grown on each plate in 1 mL of DMEM supplemented with 10% FBS. After incubation at 37℃ for 40 h, adhered cells were quantified

using the CCK-8 kit. Absorbance at 450 nm was measured using a spectrophotometric microplate reader (V-650; Jasco).

**Enzyme-linked immunosorbent assay**

Enzyme-linked immunosorbent assays (ELISAs) were performed for quantitative analysis of the expression of α-smooth muscle actin (α-SMA) and matrix metalloproteinase-2 (MMP-2) in fibroblasts on ePTFE plates. The fibroblast-adhered ePTFE plate was washed thoroughly and then incubated in fresh medium for 24 h. Subsequently, the medium was collected and centrifuged at 3000 rpm for 15 min. The supernatant was immediately analyzed using the ELISA kit in accordance with the manufacturer's protocol. Protein standards and culture medium samples were added to the ELISA plates and incubated for 1 h at 37℃. Absorbance at 450 nm was measured using a spectrophotometric microplate reader (V-650; Jasco).

**Bacterial attachment test**

*S. aureus* (ATCC 29213) was donated by the Asan Medical Center (Seoul, Korea). The bacteria were incubated in brain heart infusion broth (BHI) at 37℃ for 24 h prior to the attachment test. Each ePTFE plate was incubated for 24 h at 37℃ in a suspension of *S. aureus* (1 mL) in the BHI medium with an initial optical density ($OD_{600}$) of 1.0. After incubation, the surface of the ePTFE plate was washed thoroughly with fresh DPBS. Attached bacteria were stained with a Live/Dead BacLight solution (Invitrogen, Thermo Fisher Scientific) for 15 min. After staining, plates were washed with DPBS (×3). Fluorescence images

were obtained using a confocal laser scanning microscope (LSM 880; Carl Zeiss, Oberkochen, Germany) at an excitation wavelength of 488 nm and an emission wavelength of 520 nm. Five microscope images (140 × 140 μm) were analyzed using an image analysis program (ZEN 2012; Blue Edition, Germany) to measure the fluorescence intensity for each sample. The number of bacteria on the ePTFE surface was further analyzed by counting colony forming units (CFU). For this analysis, the ePTFE plates incubated in BHI medium were transferred to fresh medium after DPBS washing. After incubation for 6 h at 37℃, the medium was diluted and placed on BHI agar plates. After subsequent incubation at 37℃ overnight, the number of colonies was counted to determine the number of live bacteria.

**Preparation of animals**

Female Sprague–Dawley rats aged 10 weeks with a body weight of 320–340 g at the time of implantation were used. The rats were housed in an animal facility and treated in accordance with the Guide for the Care and Use of Laboratory Animals of Seoul National University Boramae Hospital. This study was approved by the Institutional Animal Care and Use Committee (IACUC) of the Seoul National University Boramae Hospital (IACUC No. 2014-0018). The animals were anesthetized by an intraperitoneal injection of Zoletil and Rumpun (50 mg/kg and 5 mg/kg, respectively) and injected with cefazolin (60 mg/kg) as a prophylactic antibiotic in the supine position. The back lesions were shaved, sterilized with a 10% povidone-iodine solution, and draped for implantation.

**Insertion and harvesting of the ePTFE plates**

Two separate 2-cm vertical incisions were made on the back of each rat through the center, beginning at the lateral point 1.5 cm from the midline and 1.0 cm below the shoulder bone. After the minimal dissection, non-grafted ePTFE and PMPC-grafted ePTFE plates were inserted beneath the left and right panniculus carnosus muscle, respectively. The muscle incisions were closed with 4-0 Vicryl® (Johnson & Johnson, New Brunswick, NJ, USA) and the skin incisions were sutured using 5-0 Ethilon® (Ethicon, Inc., Somerville, NJ, USA). The rats were placed in cages at 21–24℃ and 50–60% humidity with a 12 h-light/dark cycle and fed freely with standard laboratory rat food and water. At each time point of 24 and 72 h, eight rats were sacrificed by $CO_2$ asphyxiation following the American Veterinary Medical Association (AVMA) guidelines, respectively. At each of 4 and 12 weeks, nine rats were sacrificed. The tissue near the implanted ePTFE plate was retrieved through a skin incision.

**Histological analysis**

Harvested tissue samples were fixed in a 10% neutral formalin solution, embedded in paraffin, and cut into sections with a thickness of 4 mm. For the histological analysis, each sample slide was stained with hematoxylin and eosin (H&E). The H&E-stained slides were viewed on a conventional light microscope at low magnification (×100) to identify inflammatory areas in each section by a single pathologist (GJM). Four representative areas were then randomly selected in each slide image and analyzed at high magnification (×400) to count the number of immune cells. The number of immune cells per

unit area (1 $mm^2$) was derived from the numbers of cells in the four highly magnified representative areas of each slide. Therefore, at 24 and 72 h, 16 areas per group (4 animals × 4 areas) were analyzed in total. At 4 and 12 weeks, 36 areas per each group (9 animals × 4 areas) were analyzed in total. Immunohistochemical staining was performed using rabbit anti-transforming growth factor (TGF)-β (1:100; Abcam, Cambridge, UK) and rabbit anti-myeloperoxidase (MPO) (1:200; DAKO, USA) antibodies, in accordance with the manufacturers' protocols. Virtual microscope scanning of the slides was performed to determine the immunohistochemical staining intensity using Aperio ScanScope (Aperio Technologies, Vista, CA, USA), and TGF-β-and MPO-positive cells were counted following the same methods as used for the H&E examination.

**Cytokine assays**

At 24 and 72 h, harvested tissue samples (0.1 g) were suspended in phosphate-buffered saline (PBS) (1 mL) supplemented with 0.05% Tween-20 and 1% PIC. After mechanical homogenization at 1000 rpm for 5 min on ice, the suspension was centrifuged at 3000 rpm for 10 min at 4℃. The sorted supernatants were stored at −80°C before the cytokine analysis. The concentration of total soluble proteins was evaluated using the BCA Protein Assay Kit. The amount of cytokines was analyzed using multiplex cytokine analysis kits [CINC-3/CXCL2, interferon (IFN)-γ, IL-1B/IL-1F2, IL-6, TNF-α, GRO/KC/CINC-1, and IL-17A]. Data were collected with Luminex 100 (Luminex, USA), and analyzed with the MasterPlex QT V.2.0 (MiraiBio,

USA). All assays were performed in duplicate in accordance with the manufacturer's protocol. The cytokine level is expressed as the value relative to the total amount of protein.

**Statistical analysis**

Data are expressed as mean ± standard error of the mean (S.E.M.). GraphPad Prism (version 5.00 for Windows; GraphPad Software, La Jolla, CA, USA) was used to analyze data. Unpaired *t*-tests were performed to determine significant differences among groups, assuming a Gaussian distribution of the sample values. When the *p*-value was less than 0.05, a significant difference was accepted. Differences are presented on graphs as *, **, ***, and ****, which indicate $0.01 \leq p < 0.05$, $0.001 \leq p < 0.01$, $0.0001 \leq p < 0.001$ and $p < 0.0001$, respectively. 'No SD' means that there was no significant difference.

# Results

**Surface grafting of the ePTFE plate with PMPC**

The surface of ePTFE plates was grafted with PMPC by a two-step procedure. The surface was partially reduced by NaH[30] and then MPC monomers were polymerized with cross-linking on the reduced ePTFE surface (Figure 2).

The dynamic water contact angle results show the hydrophilic characteristics of the PMPC-grafted surface (Figure 3, 4). The advancing and receding water contact angles of the non-grafted ePTFE surface were 134° and 126°, respectively, but those of the PMPC-grafted surface were 34° and 20°, showing a dramatic increase in the hydrophilicity of the surface by the addition of the PMPC grafting.

To confirm the existence of PMPC polymers on the surface of the ePTFE plate, a surface elemental analysis was performed by XPS (Figure 5). The PMPC-grafted ePTFE surface showed P and N signals, which supported the presence of phosphorylcholine moieties of PMPC polymers on the surface. Non-grafted ePTFE showed two C1*s* peaks, a C-C peak (285 eV) and a C-F peak (292 eV). After grafting with PMPC, the intensity of the C-F peak was greatly reduced, and new peaks for C-O (286 eV) and C=O (289 eV) were observed. The presence of ester groups in the MPC monomeric unit was confirmed by the peaks. In addition, the increase in the O1*s* peak and the reduction in the F1*s* peak indicated an increase in the O content and decrease in the F content on the surface of ePTFE upon grafting with the PMPC polymer.

The quantitative analysis of the XPS peaks is summarized in Table 1. The F/C ratio was decreased from 2.03 to 1.39 by the reduction process, supporting the defluorination reaction and the partial exchange of F to H. After successive PMPC polymerization following the reduction, the F/C ratio was further decreased to 0.48 and the content of N, P, and O was greatly increased, supporting that PMPC was successfully grafted on the ePTFE surface.

In addition, the presence of phosphorylcholine moieties on the PMPC-grafted ePTFE surface was confirmed by FT-IR (Figure 6). Non-grafted ePTFE showed a simple FT-IR spectrum with two characteristic peaks at 1211 and 1154 $cm^{-1}$, which correspond to the vibration modes of $CF_2$ symmetric stretching.[31] However, the PMPC-grafted ePTFE showed additional peaks at 970 and 1080 $cm^{-1}$, corresponding to the vibration modes of P-O, and at 1720 $cm^{-1}$, corresponding to C=O vibration, all of which are characteristic peaks of phosphorylcholine moieties.

**Surface morphology of the ePTFE plates**

ePTFE, the expanded form of PTFE, has micrometer-sized pores with gas molecule penetrability. As shown in the SEM image (Figure 7A), PTFE fibers with a thickness of 50–100 nm were interconnected to form densely packed networks with pores of size 10–30 μm. After PMPC grafting, the thickness of the fiber increased to 100–200 nm, indicating the grafted polymers on the surface (Fig. 7B). However, the overall morphology of the fiber networks was maintained during the coating process. In addition, micrometer-sized pores

were also maintained after grafting, without substantial changes in size and morphology.

**Protein adhesion on the PTFE plates**

The effect of PMPC grafting on protein adsorption was evaluated by quantifying the surface proteins. BSA and BPF were selected as representative proteins to analyze protein adsorption on the implant surface. Instead of the ePTFE plate, a non-expanded PTFE plate with the same dimensions was used to quantify protein adsorption; more accurate results were expected without the effects of the porous network structure during the washing process to remove non-adsorbed proteins. Although no significant difference was observed in BSA adsorption between non-grafted and PMPC-grafted surfaces (Figure 8A), a 40% reduction in BPF adsorption was observed on the PMPC-grafted plate compared with that on the non-grafted plate (Figure 8B).

**Adhesion and activation of fibroblasts on the ePTFE plates**

I evaluated cell adhesion on the PMPC-grafted ePTFE plates. The adhesion of fibroblasts (NIH3T3), which are important for capsular formation around the implants, was quantified using a CCK assay (Figure 10A). There were 50% fewer adhered fibroblasts on the PMPC-grafted ePTFE than on the non-grafted ePTFE. The adhesion of fibroblasts on the ePTFE plate was thus inhibited by PMPC grafting. In addition, the activation level of adhered fibroblasts was measured by ELISAs of matrix metalloproteinase-2 (MMP-2) and α-smooth muscle actin (α-SMA) (Figure 10B). The expression levels of MMP-2 and α-

SMA were reduced on the PMPC-grafted ePTFE surface by 20% and 30%, respectively.

**Adhesion of bacterial cells on the ePTFE plates**

Bacterial adhesion was also significantly influenced by PMPC grafting (Figure 11). As shown in the fluorescence microscopic images (Figure 11A), *S. aureus*, an important causal bacterium in inflammation and infection during implantation, adhered and grew on the ePTFE plates. Strong green BacLight dye fluorescence was clearly observed between the PTFE fibers. However, significantly reduced fluorescence intensity was observed on the PMPC-grafted ePTFE plates (Figure 11B). Based on the quantitative fluorescence intensity results, PMPC grafting could reduce bacteria on the surface by more than 60% (Figure 11C). In addition, the adhered bacterial cells were quantified by colony forming unit (CFU) counting. The ePTFE plates that had been pre-incubated in bacteria-containing medium were transferred to fresh medium without bacteria and incubated for an additional 6 h. The resulting CFU of the medium after further incubation on an agar plate indicated the initial numbers of bacteria adhered on the ePTFE surfaces. The level of bacteria was reduced from $4.3 \times 10^7$ CFU/cm$^2$ to $1.3 \times 10^7$ CFU/cm$^2$ on the PMPC-grafted ePTFE (Figure 11D).

**In vivo capsular formation around ePTFE plates and cell infiltration**

Tissues around the ePTFE plates were collected at 4 and 12 weeks after implantation in the backs of Sprague–Dawley rats (Figure 13). Microscopic images of H&E-stained tissues are shown at 4 weeks (Figure 14) and at

12weeks (Figure 15). No thick fibrous capsular tissue was observed around non-grafted and PMPC-grafted ePTFE plates (Figure 14, 15).

Nuclei of various inflammation-related cells, such as myeloid and lymphoid cells, are generally observed as blue dots in H&E images. In the deep fiber region of ePTFE plates, almost no inflammatory cells were detected. However, the infiltration of inflammatory cells was observed near the edge of the ePTFE fibers (Figure 14C–D, 15.C–D). Figure 15E shows a quantitative comparison of inflammatory cells in the edge fiber region of the ePTFE plates after 4 and 12 weeks. Between the two time points, the number of infiltrated inflammatory cells increased by 2–3 times. Although no significant difference was observed at 4 weeks, a nearly 35% reduction in inflammatory cells was observed in the PMPC-grafted plate compared with that in the non-grafted plate at 12 weeks.

**Immunohistochemical analysis of tissues around the ePTFE plates**

Immunohistochemistry (IHC) was performed to examine the inflammatory reaction around the ePTFE plate in greater detail. Transforming growth factor-β (TGF-β), a main growth factor secreted from various inflammatory cells, and myeloperoxidase (MPO), an important peroxidase enzyme mainly expressed in myeloid cells, were selected as representative inflammatory markers.

Figure 16 shows IHC images and a quantitative comparison of TGF-β in the non-grafted ePTFE and PMPC-grafted ePTFE groups. Similar to the H&E staining results, TGF-β was mainly detected near the edges of ePTFE fibers (Figure 16A–D, Figure 17A–D). The level of TGF-β expression decreased between 4 and 12 weeks (Figure 17E). At both time points, a 40–50% reduction

in TGF-β expression was observed in the tissues around the PMPC-grafted ePTFE plates compared with that in the non-grafted plates.

Figure 18 shows IHC images and a quantitative analysis of MPO expression. Again, MPO expression was quite concentrated in the edge region (Figure 18A–D, 19A–D). The time course of MPO expression was quite similar to that of TGF-β (Figure 19E). MPO levels decreased between the two time points. The tissues around the PMPC-grafted ePTFE plates showed a reduction of approximately 40% in MPO expression compared with the tissues around the non-grafted plate.

**Analysis of acute inflammatory reactions around the ePTFE plates**

Acute inflammatory reactions around the ePTFE plates were analyzed using multiplex cytokine analysis kits at 24 and 72 h after implantation. Among various cytokines including IFN-γ, IL-1b, IL-6, TNF-α, CSCL1, CXCL2 and IL-17a, only IL-6 and TNF-α were detected at measureable levels. The amounts of IL-6 and TNF-α slowly decreased during the period between 24 and 72 h (Figure 20). However, almost no significant differences in both cytokines were observed between non-grafted and PMPC-grafted ePTFE.

In the H&E and IHC analyses, the number of inflammatory cells increased slightly (Figure 21A), but the levels of TGF-β and MPO expression decreased during the period. A lower level of TGF-β expression was observed in the PMPC-grafted plate than in the non-grafted plate at both time points (Figure 21B). A lower level of MPO in the tissues around the PMPC-grafted plate was only observed at 72 h (Figure 21C).

# Discussion

High physical and chemical stability of PTFE polymers can be a drawback for the physical or chemical modification of ePTFE surfaces because materials physically adsorbed on the ePTFE surface are easily removed by mechanical shearing forces owing to the low surface energy.[2] Additionally, C–F bond functionalization with other reactive groups is difficult.[30,32] In this research, i wanted to introduce zwitterionic biomembrane-mimic polymers on the ePTFE surface in a semi-permanent manner. Covalent grafting is preferred for the stable immobilization of zwitterionic polymers, but covalent bond formation on chemically inert PTFE polymers was difficult.

The 'grafting-from' strategy can provide the polymer-coated surface with high grafting density, but reactive species should be generated on the target surface to initiate the grafting.[33] Photo-initiated radical formation followed by propagation is a well-developed method for densely packed polymeric grafts.[19] Acrylate- or methacrylate-based polymers are easily polymerized on the surface by UV irradiation in the presence of photoinitiators.[19,24] However, polymer grafting on the intact ePTFE surface was ineffective using the direct grafting strategy; accordingly, the C-F bonds of the PTFE polymer should be partially reduced to C-H bonds (Figure 4). UV-irradiated BP can generate various reducing intermediates such as diphenyl ketyl radical anion or benzhydrol anion by electron transfer from NaH, and the produced intermediates can successively defluorinate the surface to form C-H bonds (Figure 2).[30] The partially reduced PTFE polymer can generate reactive radicals

on the surface more efficiently in the presence of BP by UV irradiation than the intact PTFE polymer. The triplet state of UV-irradiated BP can abstract a hydrogen atom from the C-H bond to generate a reactive radical for polymer grafting.[19]

PMPC grafting was confirmed based on the water contact angle on the non-expanded PTFE surface without the porous structure of ePTFE. Effective hydration and high hydrophilicity are well-known properties of zwitterionic PMPC polymers.[22,34,35] I expected that solvophobic PTFE surfaces became hydrophilic surfaces by PMPC grafting. To enhance the PMPC grafting efficiency, i used additional cross-linkers with several polymerizable acrylate groups. I expected the cross-linkers to form a polymeric network between grafted PMPC chains and increase the coating efficiency and durability.[36] The comparison among the PTFE surfaces after various treatments clearly showed that the grafting with the cross-linkers on the reduced PTFE provided a much more hydrophilic surface than other methods (Figure 4). Based on these results, i used the same protocol for surface grafting on ePTFE with a porous structure, and successfully prepared PMPC-grafted ePTFE plates, as confirmed by analyses of the water contact angle (Figure 3), XPS (Figure 5 and Table 1), and FT-IR (Figure 6). The similar surface properties of PMPC-grafted non-porous PTFE and porous ePTFE indicate that PMPC immobilization is not induced by the molecular entanglement of PMPC polymers with the porous ePTFE network, but by the efficient 'grafting-from' mechanism on the ePTFE surface. I used the PMPC-coated ePTFE plates for further experiments *in vitro* and *in vivo*.

High gas permeability and other attractive mechanical properties of ePTFE as a platform material for biomedical implants are largely attributed to the porous structure of the fabric. Pore sizes from 10–30 μm can be a barrier against the irregular ingrowth of most eukaryotic cells, including fibroblasts.[2,37] Capsular contracture, the formation of thick fibrous tissue around foreign implants, was significantly inhibited around the ePTFE implants compared with that in other material-based implants.[38,39] In addition, the infiltration of extracellular matrix into the porous structure can inhibit the irregular migration of implants from the targeted location.[37] Even after PMPC grafting, the porous structure was maintained, as shown in the SEM images (Figure 7). The thickness of the PTFE fiber increased by 50–100 nm, indicating that the thickness of the PMPC layer was approximately 25–50 nm. The SEM images also indicated that PMPC was uniformly grafted on the PTFE fibers. I also compared two important mechanical properties, namely, Young's modulus and tensile strength, between non-grafted ePTFE and PMPC-grafted ePTFE (Table 2). The characteristic stiffness and tensile strength of ePTFE, which was initially modulated by the manufacturer, were nearly unchanged by PMPC grafting.[40] The maintenance of pore morphology, Young's modulus, and tensile strength suggests that our grafting strategy does not have harmful effects on the beneficial mechanical properties of ePTFE for biomedical applications.

I expected PMPC grafting to inhibit nonspecific protein adsorption on the ePTFE surface. Structural changes in adsorbed proteins can provoke foreign body reactions, including inflammation.[2,6] Moreover, bacteria and fibroblasts, which play essential roles in infection and thick fibrous tissue formation,

respectively,[28,29] may adhere on the implant surface via adsorbed proteins.[41,42] Zwitterion polymers generate effective hydration layers around the electronic dipole of zwitterionic residues, such as carboxybetaine, sulfobetaine, or phosphobetaine, and inhibit nonspecific interactions with other hydrophobic or hydrophilic molecules in aqueous solutions.[16,43] In particular, PMPC mimicking the head group of phosphatidylcholine in the plasma membrane shows an exceptional ability to inhibit protein adsorption, thrombosis, and fibrosis.[24,25,44] In addition, successful *in vivo* results for PMPC-coated coronary stents[20,21] and artificial joints[23] support the choice of PMPC as the grafting polymer on the ePTFE implant.

I quantified protein absorption on the non-expanded PTFE plate, instead of the ePTFE plate, to obtain accurate estimates of the effect of PMPC grafting on the outermost surface. Figure 8A shows that PMPC grafting reduced BSA adsorption on the PTFE surface slightly, but this effect was not significant. In contrast, as shown in Figure 8B, BPF adsorption was reduced by 40% by PMPC grafting. These results indicate that PMPC grafting can inhibit serum protein adsorption on the PTFE surface, but the inhibitory activity is dependent on protein characteristics. It has been suggested that albumin adsorption can improve the biocompatibility of artificial materials.[45] However, fibrinogen adsorption mediates plasma clotting and foreign body reactions on the surface of artificial materials.[2,41,42] Therefore, more effective reductions in BPF adsorption compared to BSA adsorption on the PMPC-grafted surface might increase the biocompatibility of PTFE-based implants. Since protein adsorption was not reduced on reduced PTFE without PMPC grafting (Figure 9), the anti-

adsorptive effect was clearly due to the PMPC polymers on the surface of the PTFE plate.

The reduction in protein adsorption on the PTFE surfaces caused the inhibition of eukaryotic and bacterial cell adhesion (Figure 10, 11). Mouse fibroblast cells showed 50% less adhesion on the PMPC-grafted ePTFE than on the non-grafted type (Figure 10A). As over a 60% increase of fibroblast adhesion was observed on the reduced ePTFE plate without the PMPC grafting (Figure 12), the decrease of fibroblast adhesion on the PMPC-grafted ePTFE was mainly due to the PMPC grafting. This reduction in fibroblast adhesion is expected to alleviate the formation of thick and irregular fibrous capsules around the implant surfaces.[24] Moreover, the expression level of two representative proteins of activated fibroblasts, MMP-2 and α-SMA, decreased on the PMPC-grafted ePTFE surface by 20% and 30%, respectively (Figure 10B). Since MMP-2 plays an important role in epithelial cell migration[46] and α-SMA is an indicator of collagen maturation[24] the lower expression of both proteins partially supported that fibroblasts on the PMPC-grafted ePTFE surface might be less activated than those on the non-grafted ePTFE surface.

Although the porous structure of ePTFE could be beneficial for reduction of the irregular ingrowth of thick fibrous tissues, it may provoke the most frequent complications associated with ePTFE implants: infection and inflammation.[6,39] Bacteria with a size of 0.5–1.5 μm can easily infiltrate the pores of ePTFE, which are 10–30 μm in size, but macrophages and natural killer cells cannot easily penetrate the pores, enabling the survival of infiltrated bacteria and

causing serious infection.[2] *S. aureus* is one of the major pathogenic bacteria that cause infection and inflammation after implantation surgery; accordingly, i examined the adhesion and growth of the bacteria on the PMPC-grafted ePTFE. As shown in Figure 11A, *S. aureus* cells adhered and grew actively within the porous network structure of non-grafted ePTFE plates. However, the bacteria were reduced by over 60% on the PMPC-grafted plates (Figure 11B–D). As the porous network structure of ePTFE was still intact in the PMPC-grafted ePTFE (Figure 7B), i inferred that the reduction in bacterial adhesion was mainly a consequence of the PMPC polymer on the surface. In addition, the bacterial adhesion and growth tests were performed in extremely bacterium-rich conditions (Materials and Methods); therefore, i expected that PMPC grafting could effectively inhibit bacterial adhesion and growth in real implantation conditions with very low densities of bacteria.

Finally, to demonstrate the anti-inflammatory effect of PMPC grafting on the ePTFE surface, i implanted non-grafted and PMPC-grafted ePTFE plates in the back of rats (Figure 13). Although the biological environment around the implants is varied according to the ePTFE application, i focused on the relationship between PMPC coating on the ePTFE and inflammation in the simple animal model. After artificial material implantation, foreign body reactions, including inflammation and fibrous capsular formation, are generally provoked, along with wound healing procedures.[47] After wound healing was stabilized, tissue specimens surrounding the implanted ePTFE plates were harvested at 4 and 12 weeks. As shown in Figure 14 and 15, no sign of thick fibrous capsular formation was observed around non-grafted or PMPC-grafted

ePTFE plates. In previous studies, negligible or thinner fibrous capsules formed around ePTFE implants compared with those around silicone- or collagen-based implants.[48] The intrinsic characteristics of ePTFE might inhibit extensive capsular formation around the implant.

The expression levels of two main inflammation-related factors, TGF-β and MPO, were used as indicators of inflammation. TGF-β is an important cytokine secreted from most leukocytes, activating lymphocytes, and macrophages to boost inflammation.[49] Most TGF-β-positive cells were observed near the edges of the ePTFE plates (Figure 16, 17). This observation supports the inference that it is difficult for leukocytes to penetrate the porous network of ePTFE. The gradual decrease in TGF-β expression between 4 and 12 weeks indicates that inflammation was alleviated during this period (Figure 17E). More importantly, the number of TGF-β-positive cells was clearly 40%–50% lower in the tissues around the PMPC-grafted ePTFE than in the non-grafted ePTFE at both time points. MPO is a lysosomal enzyme that is mostly expressed in myeloid cells, such as neutrophils or monocytes.[50] MPO plays an important role in antimicrobial activity by mediating phagocytosis, particularly in acute inflammation. Similar to TGF-β expression, MPO expression decreased between 4 and 12 weeks (Figure 18, 19). Additionally, an approximately 40% reduction in MPO levels was observed on the PMPC-grafted ePTFE (Figure 19E). The two main indicators of inflammation were

clearly reduced by PMPC grafting, indicating an anti-inflammatory effect of the PMPC-grafted surface. Because structural changes in adsorbed proteins can initiate foreign body reactions, the inhibition of non-specific protein adsorption (Figure 8) and protein denaturation[10,41,42] could contribute to the alleviation of inflammation on the PMPC-grafted surface. The anti-infection effect of PMPC-grafted ePTFE (Figure 11) could promote a reduction in inflammation in response to possible infections during implantation surgery, but this could not be directly examined in this study.

Interestingly, the total number of inflammatory cells in the H&E images increased by 2–3 times between 4 and 12 weeks (Figure 15E). We inferred that the lack of surrounding capsules around the ePTFE implants could explain this increase in total inflammatory cells. Unlike other artificial materials, including silicone, which form thick fibrous capsules for the local separation of artificial materials from host tissues,[48,51] ePTFE forms only a negligible, thin capsule (Figure 14A–B) and the surface is continuously exposed to the host immune system. We supposed that macrophages or lymphocytes, which are important inflammatory cells during the maturation phase of the wound healing process, accumulated around the ePTFE by recognizing the artificial surface. Long-term observations exceeding 12 weeks are needed to obtain a more detailed understanding of late inflammation processes. However, even at 12 weeks, the total number of inflammation-related cells was clearly reduced on the PMPC-grafted ePTFE.

Analysis of inflammatory reactions in the early stage of implantation would also be interesting. The results of multiplex assays for various inflammatory

mediators suggested that non-grafted ePTFE or PMPC-grafted ePTFE did not induce severe inflammation in the acute phase because most of the inflammatory cytokines were undetectable. Only IL-6 and TNF-α, mainly produced by macrophages,[9,41] were detected (Figure 20). The expression of these two cytokines decreased during the period between 24 and 72 h, indicating that the activation of macrophages might have been relieved. The difference between non-grafted ePTFE and PMPC-grafted ePTFE was not significant. However, the levels of TGF-β and MPO expression were clearly different, especially at the time point of 72 h (Figure 21). In both cases, PMPC-grafted ePTFE showed lower expression levels than the non-grafted one. By comparing the results at the early stage of implantation (24 and 72 h) and at the late stage (4 and 12 weeks), i suggested that the PMPC-grafted surface would affect the chronic phase of inflammation more significantly than the acute phase.

In biomedical applications, ePTFE is frequently used as a basic material in fistulas for hemodialysis and in artificial implants for reconstructive or plastic surgery. Anti-thrombotic activity is essential for the fistula and anti-bacterial or anti-inflammatory activities are clearly beneficial for implants. In this study, i developed an efficient grafting method for PMPC polymers on ePTFE, and demonstrated anti-bacterial and anti-inflammatory effects *in vitro* and *in vivo*. Combined with the well-known anti-thrombotic activity of PMPC-grafted surfaces,[52] the PMPC-grafted ePTFE could provide beneficial surface properties compared to non-grafted ePTFE for such applications.

# Conclusions

In the present study, chemically inert ePTFE surfaces were covalently grafted with a zwitterionic biomembrane-mimic polymer, PMPC, via partial reduction and successive photo-initiated polymerization in the presence of cross-linkers. PMPC grafting on the ePTFE surface effectively inhibited the adhesion of fibroblasts as well as *S. aureus*, a typical infectious bacterium during implantation, between the PTFE polymeric networks. More importantly, significant reductions in inflammation-related factors, that is, TGF-β and myeloperoxidase, were observed around PMPC-grafted ePTFE surfaces. Significant reductions in inflammation-related cells were also observed around the PMPC-grafted ePTFE, without the formation of thick fibrous tissues. PMPC grafting could provide anti-inflammatory and anti-bacterial functions to ePTFE implants, without affecting the attractive mechanical properties. Accordingly, it may be an effective solution to overcome infection and inflammation, which are the most common and serious limitations in the application of ePTFE as an implantable biomaterial.

# Figures and Tables

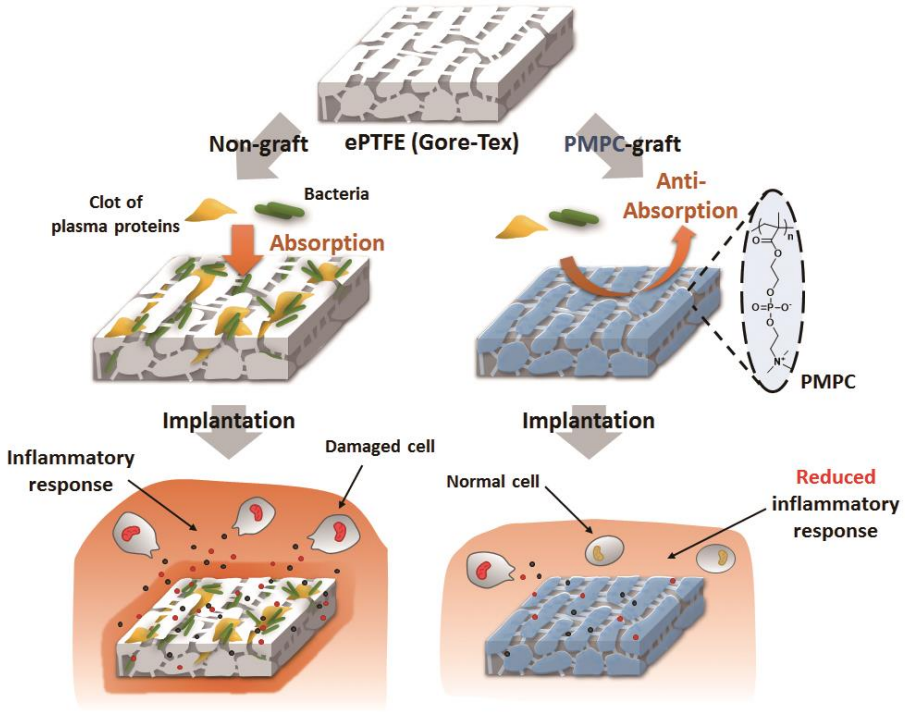


**Figure 1.** Schematic illustration of PMPC grafting on ePTFE for anti-inflammatory and anti-bacterial effects.

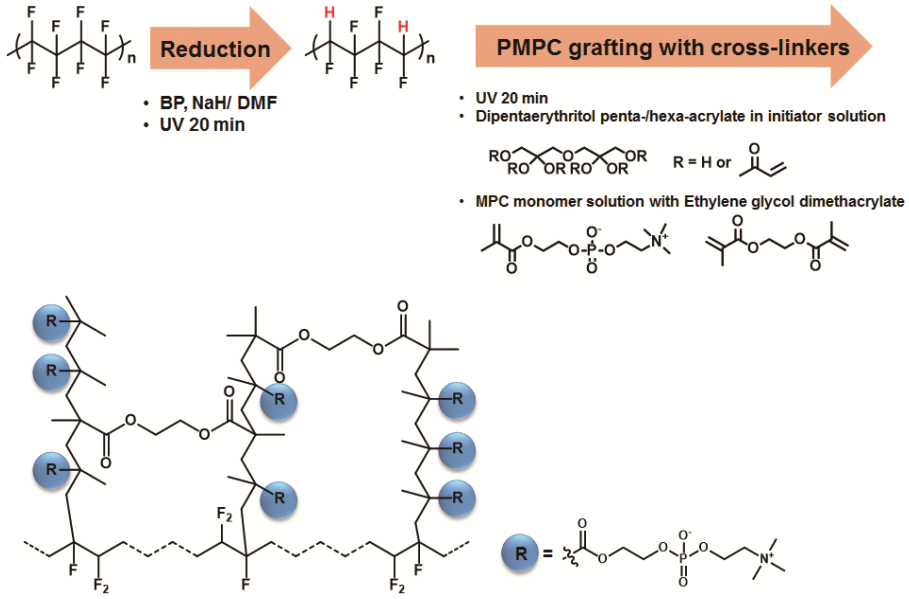


**Figure 2.** The proposed synthetic procedure of partial reduction and PMPC grafting on ePTFE surfaces. The surface of ePTFE was partially reduced by NaH and MPC monomers were polymerized with cross-linking on the reduced ePTFE surface.

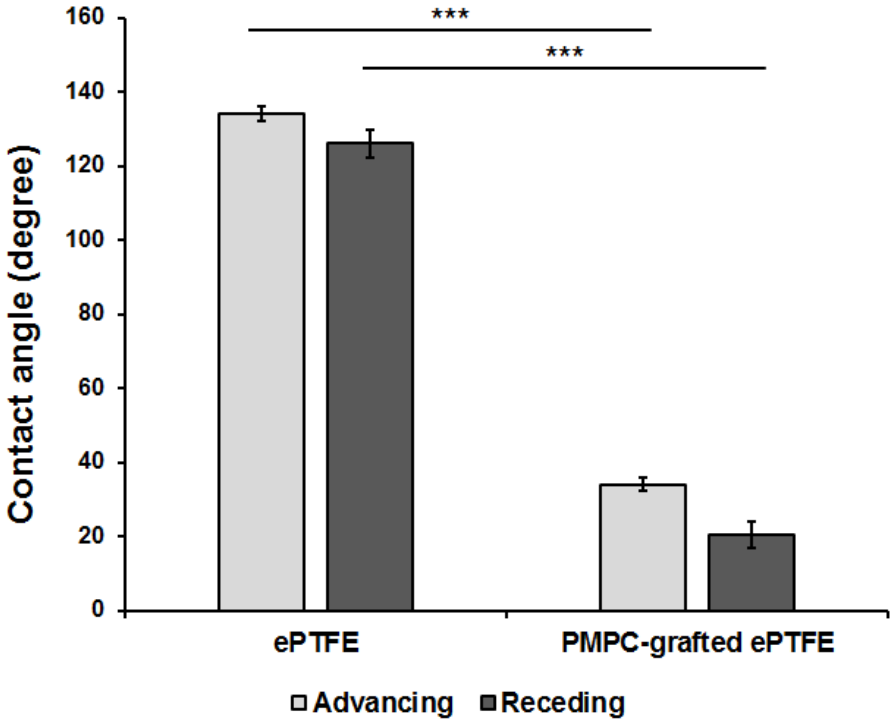


**Figure 3.** The advancing and receding water contact angles on non-grafted and PMPC-grafted ePTFE surfaces. The water contact angles of the non-grafted ePTFE surface were 134° and 126°, but those of the PMPC-grafted surface were 34° and 20°, showing a dramatic increase in the hydrophilicity of the surface by the addition of the PMPC grafting. Data are presented as mean ± S.E.M. (n = 3).

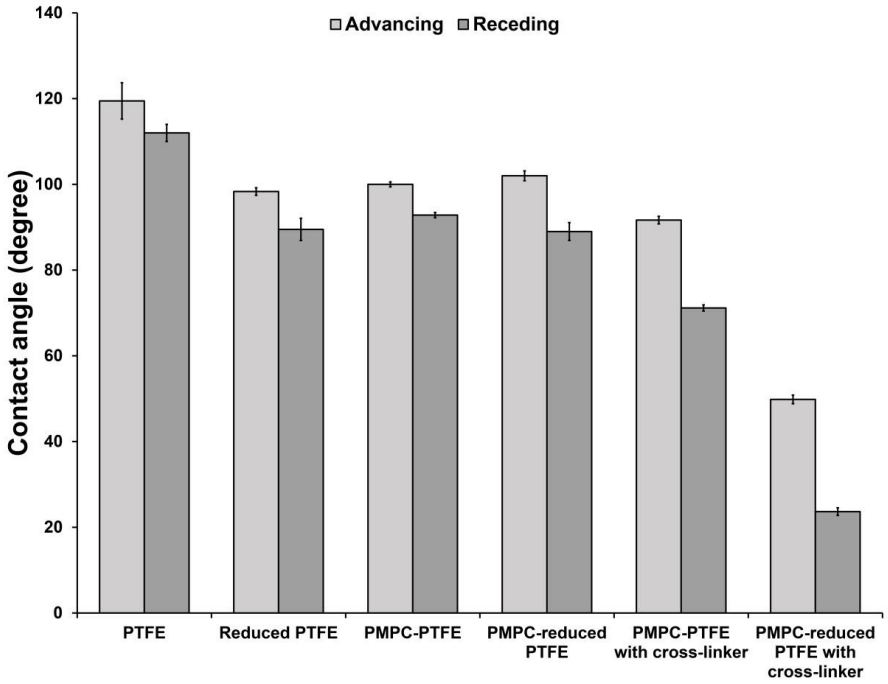


**Figure 4.** Water contact angles on PTFE plates which were surface-modified by various grafting methods. The degree of PMPC grafting was evaluated based on the water contact angle on the various non-expanded PTFE. The effectiveness of grafting was best in PMPC-reduced PTFE with cross linker through providing much more ydrophilic surface than other methods. Data are represented as mean ± S.E.M. (n = 3).

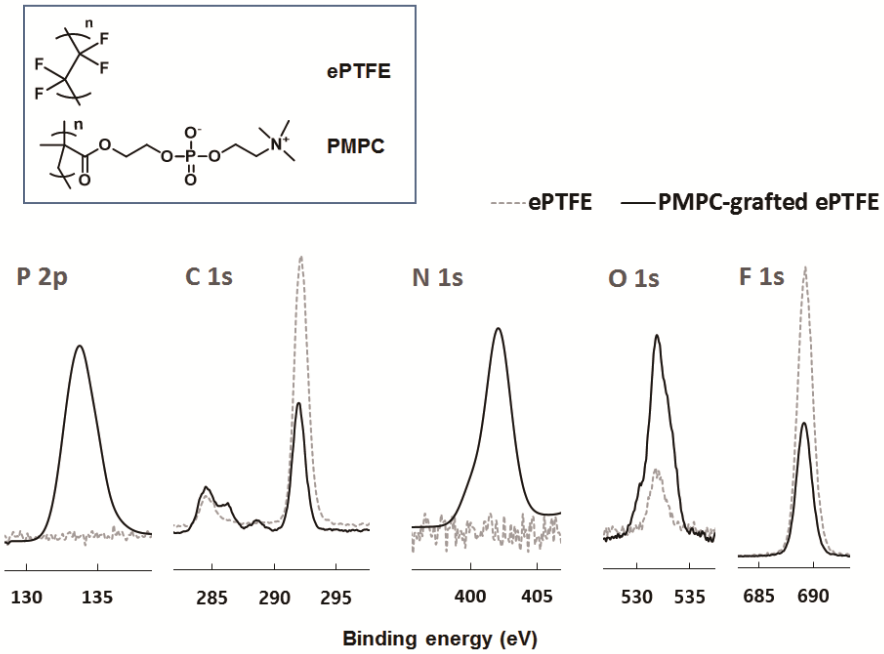


**Figure 5.** XPS spectra of non-grafted and PMPC-grafted ePTFE surfaces. The PMPC-grafted ePTFE surface showed P and N signals, which supported the presence of phosphorylcholine moieties of PMPC polymers on the surface after grafting.

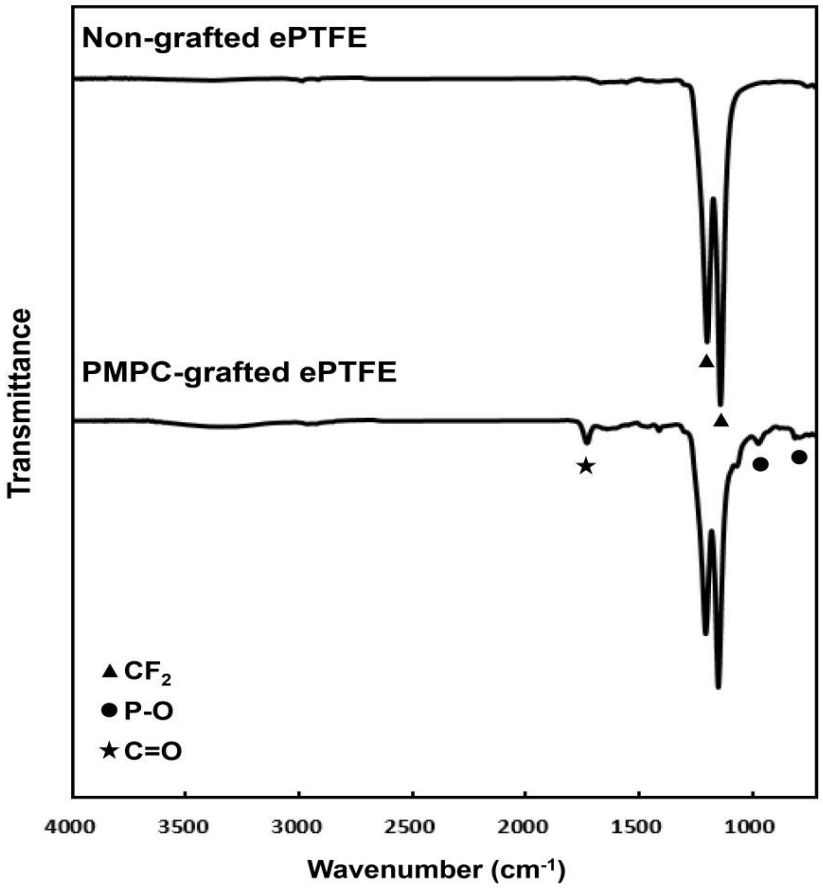


**Figure 6.** FT-IR spectra of nongrafted and PMPC-grafted ePTFE surfaces. Non-grafted ePTFE showed a simple FT-IR spectrum with two characteristic peaks at 1211 and 1154 cm−1, which correspond to the vibration modes of CF2 symmetric stretching. PMPC-grafted ePTFE showed additional peaks at 970 and 1080 cm−1, corresponding to the vibration modes of P-O, and at 1720 cm−1, corresponding to C=O vibration, all of which are characteristic peaks of phosphorylcholine moieties.

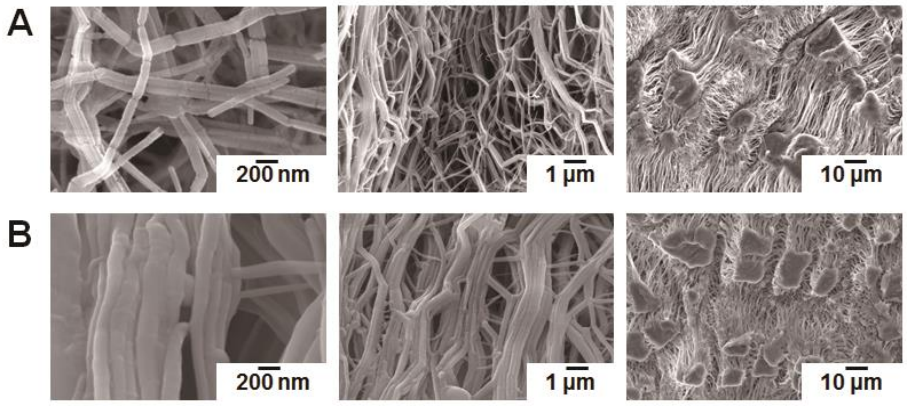


**Figure 7.** SEM images of (A) non-grafted ePTFE and (B) PMPC-grafted ePTFE surfaces. Non-grafted ePTFE (A) has micrometer-sized pores with the fiber networks. After grafting (B), overall morphology of the fiber networks and micrometer-sized pores were preserved without substantial changes in size and morphology.

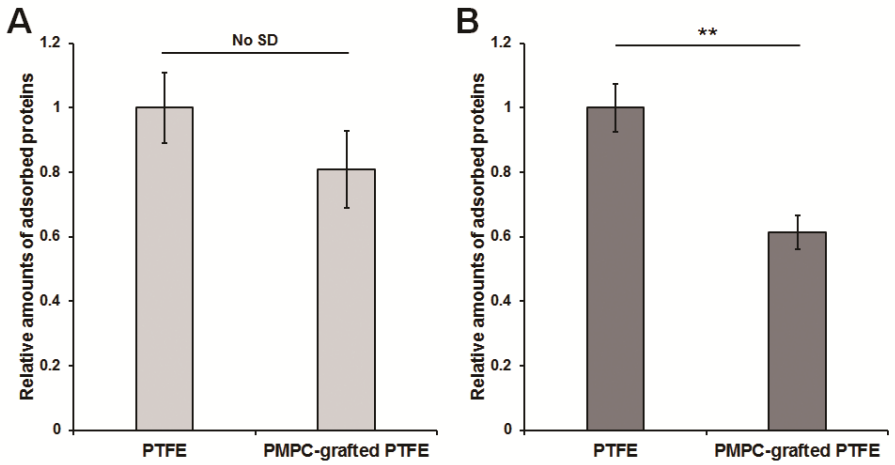


**Figure 8.** *In vitro* quantitative analysis of protein adsorption. Amounts of adsorbed (A) BSA and (B) BPF on the non-grafted PTFE and PMPC-grafted PTFE. There was no significant difference in BSA adsorption between non-grafted and PMPC-grafted surfaces (A). But there was a 40% reduction in BPF adsorption on the PMPC-grafted plate compared with that on the non-grafted plate (B). Data are presented as relative values compared with the amount of adsorbed proteins on non-grafted PTFE plate [mean ± S.E.M. (n=3)]. The amounts of adsorbed proteins on non-grafted PTFE surface were 0.22 μg/cm$^2$ and 0.44 μg/cm$^2$ for BSA and BPF, respectively, and normalized as 1.

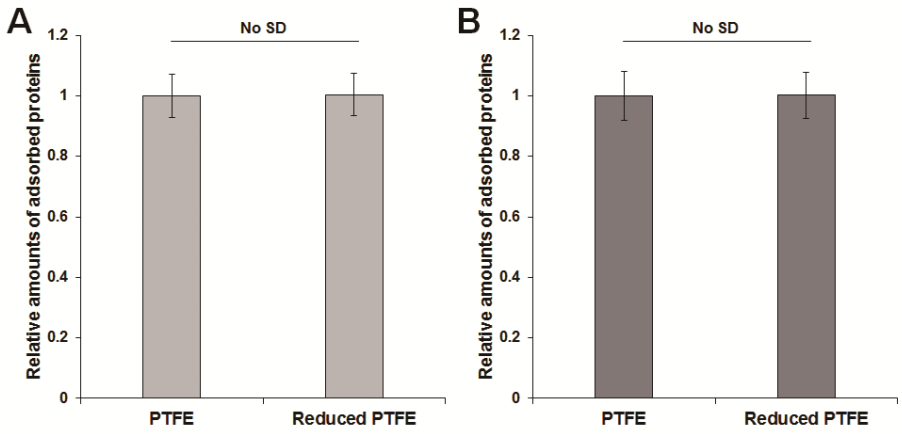


**Figure 9.** *In vitro* quantitative analysis of protein adsorption. Amount of adsorbed (A) BSA and (B) BPF on the non-grafted PTFE and reduced PTFE plate. Protein adsorptions (A, B) were not decreased on PTFE and reduced PTFE plate, respectively. Data are presented as relative values compared with the amount of adsorbed proteins on non-grafted PTFE plate (mean ± S.E.M. (n = 3)).

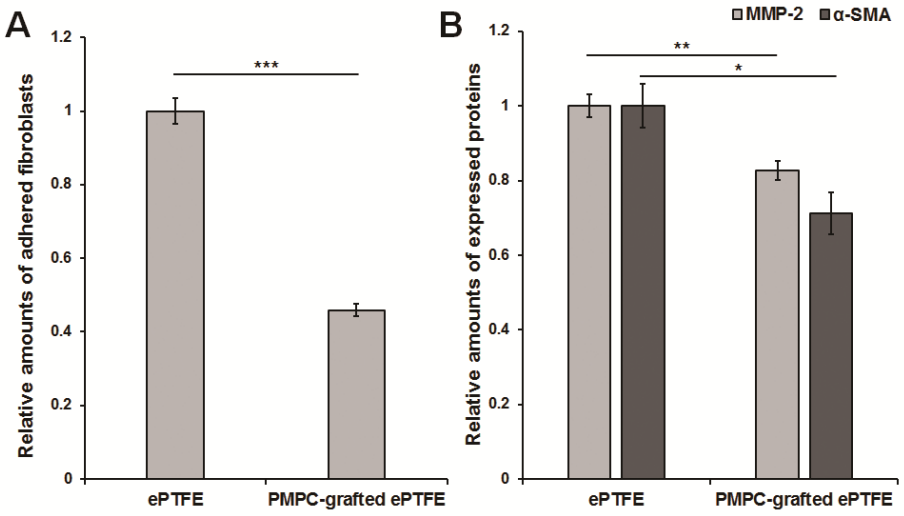


**Figure 10.** *In vitro* adhesion (A) and activation (B) of fibroblasts (NIH3T3) on non-grafted ePTFE and PMPC-grafted ePTFE plates. Adhesion of fibroblasts was 50% fewer on the PMPC-grafted ePTFE than on the non-grafted ePTFE (A). The expression levels of MMP-2 and α-SMA, representing activation of adhered fibroblasts, was reduced on the PMPC-grafted ePTFE surface by 20% and 30%, respectively (B). Data are presented as relative values compared with the amount on non-grafted ePTFE plate. Relative amounts of metalloproteinase-2 (MMP-2) and α-smooth muscle actin (α-SMA) expressed by adhered fibroblasts analyzed by ELISA. Data are presented as mean ± S.E.M. (n = 3). The amounts of expressed protein on non-grafted ePTFE surface were 2.9 ng/ml and 2.7 ng/ml for MMP-2 and α-SMA, respectively, and normalized as 1.

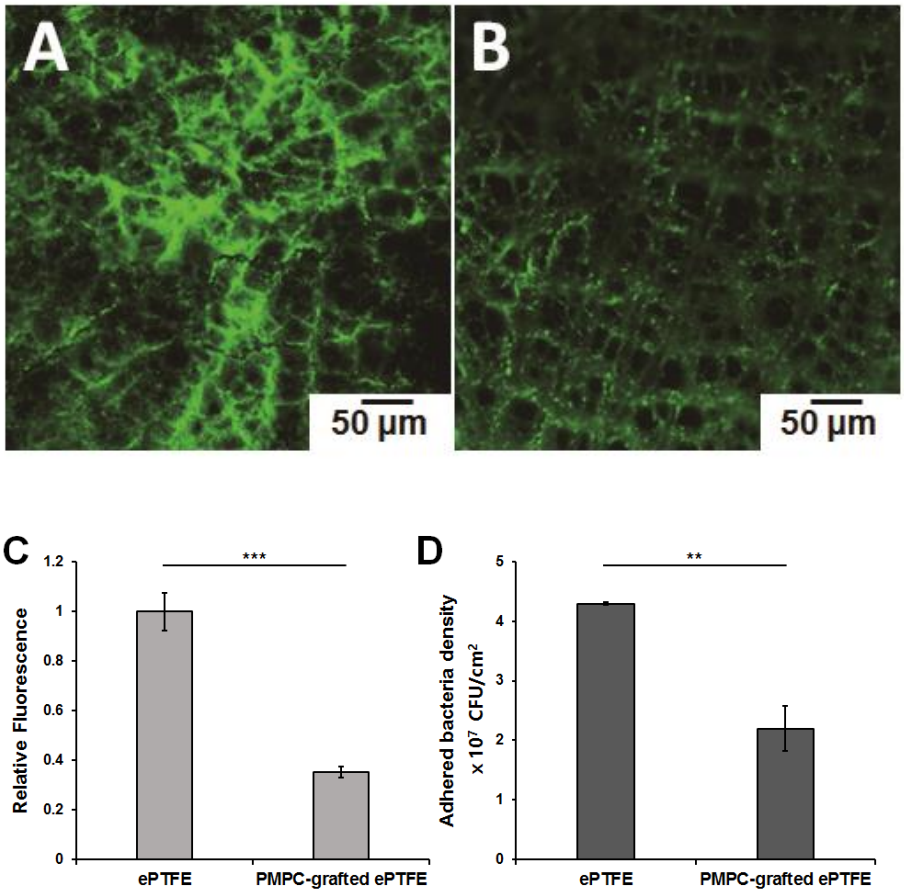


**Figure 11.** Adhesion and growth of *S. aureus* on non-grafted ePTFE (A), and PMPC-grafted ePTFE (B) plates. Quantitative analysis of bacterial amount on each sample by comparing fluorescence intensities (C) and bacterial density (CFU/cm$^2$) (D). Comparing to non-grafted ePTFE (A), significantly reduced fluorescence intensity was observed on the PMPC-grafted ePTFE (B). Quantitative analysis for fluorescence intensity and bacterial density, levels were significantly reduced in PMPC-grafted ePTFE, respectively. The bacterial density was determined by counting colony forming units (CFU) on BHI agar plates. Data are presented as mean ± S.E.M. (n = 3).

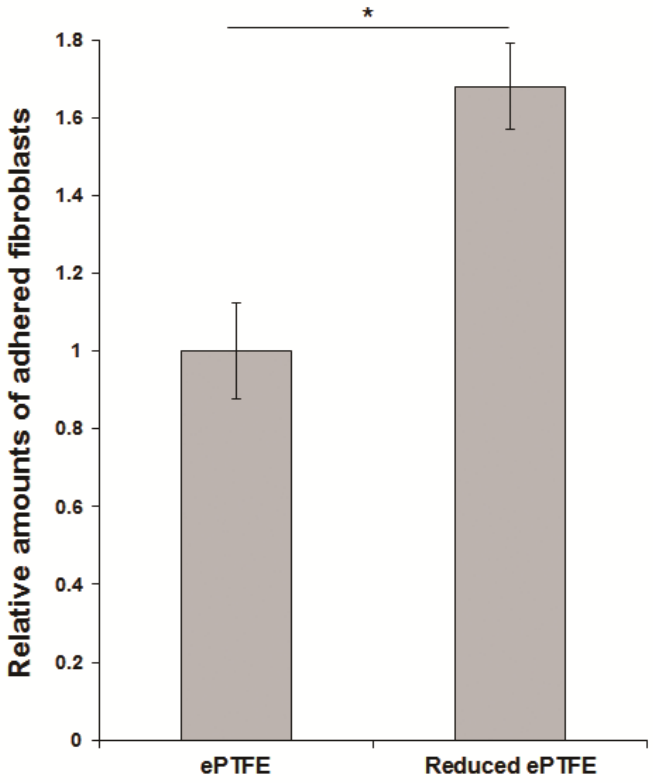


**Figure 12.** *In vitro* adhesion of fibroblasts (NIH3T3) on non-grafted ePTFE and reduced ePTFE plate. About 60% increase of fibroblast adhesion was observed on the reduced ePTFE plate without the PMPC grafting. Data are presented as relative values compared with the amount of adhered cells on non-grafted ePTFE plate. Data are presented as mean ± S.E.M. (n = 3).

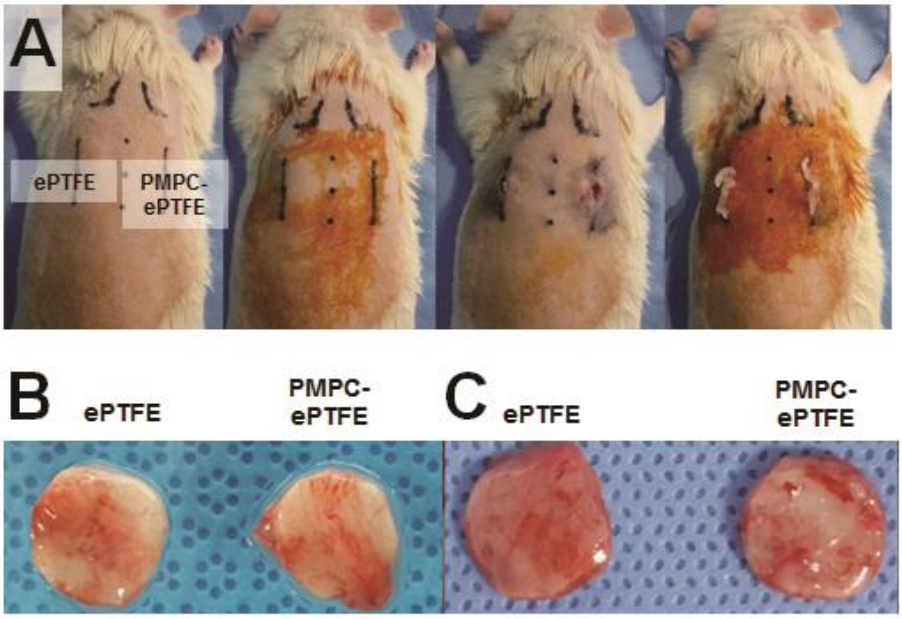


**Figure 13.** *In vivo* experiment to investigate inflammation in the tissues around non-grafted ePTFE and PMPC-grafted ePTFE implants using a rat model. Both implants were inserted into the back of rats (A). The implants were harvested with the tissues around the implants at 4 (B) and 12 weeks (C) after the insertion.

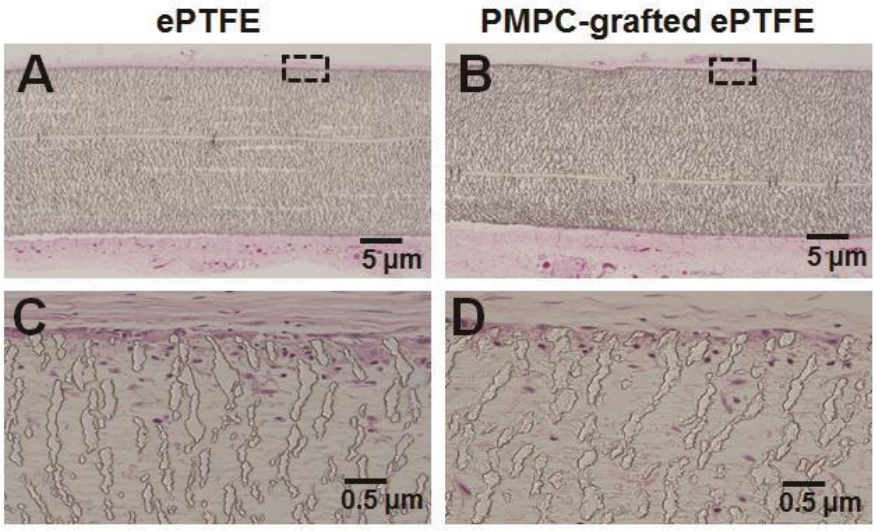


**Figure 14.** H&E staining images of tissues around the nongrafted (A, C) and PMPCgrafted ePTFE (B, D) after 4 weeks. Images with a low magnification (A, B) and images with a high magnification (C, D) for the dotted rectangles in the A and B images. Inflammatory cells were infiltrated at the edge of ePTFE plates in both groups.

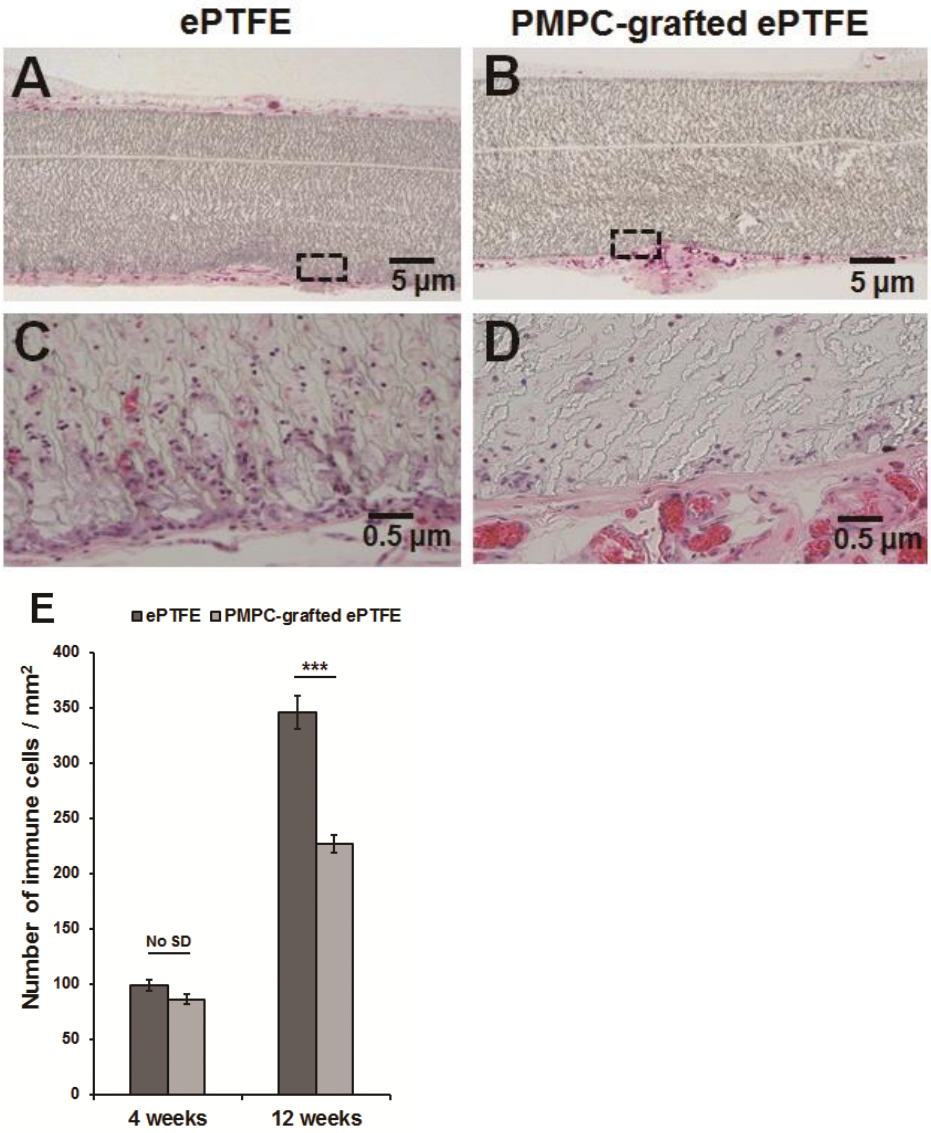


**Figure 15.** H&E staining images of tissues around the non-grafted (A and C) and PMPC-grafted ePTFE (B and D) after 12 weeks. At 12 weeks, the number of infiltrated inflammatory cells increased by 2–3 times than at 4 weeks. A nearly 35% reduction in inflammatory cells was observed in the PMPC-grafted plate compared with that in the non-grafted plate at 12 weeks. Images with a low-magnification (A and B) and images with a high magnification (C and D)

for the dotted rectangles in the A and B images. Quantitative analysis of immune cells in 36 areas (9 animals × 4 areas) of surrounding tissues (E) for each group after 4 and 12 weeks was performed. Data are presented as mean ± S.E.M. (n = 36).

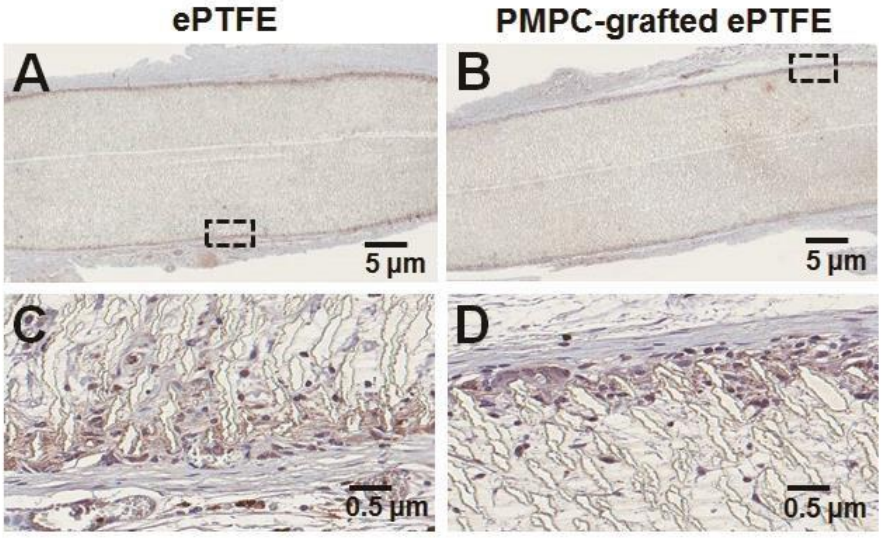


**Figure 16.** *In vivo* IHC analysis of TGF-β in the tissues around the nongrafted (A, C) and PMPC-grafted ePTFE (B, D) after 4 weeks. Images of a low magnification (A, B) and images with a high magnification (C, D) for the dotted rectangles in the A and B images. The infiltration of TGF-β positive cells was higher in the nongrafted (A, C) than PMPC-grafted ePTFE after 4 weeks.

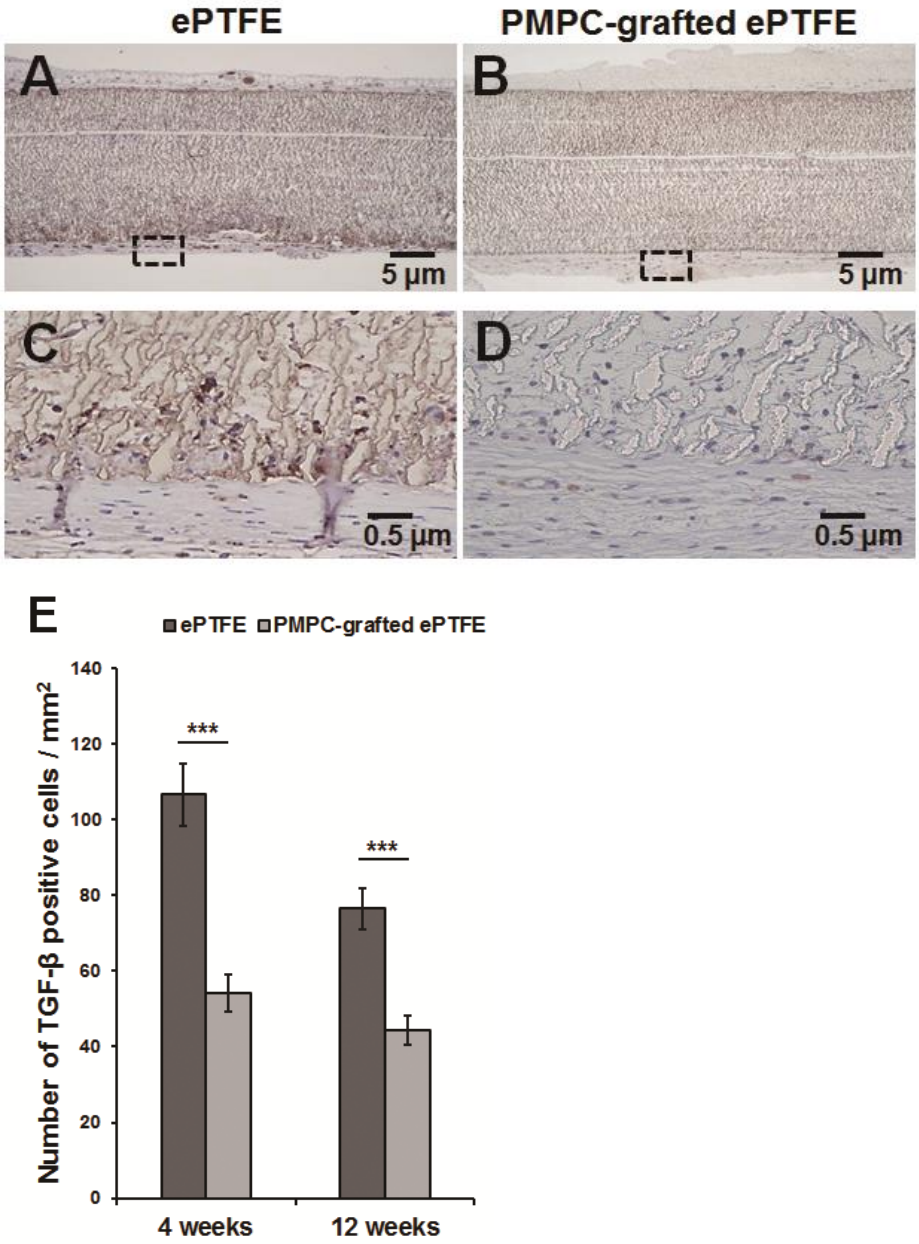


**Figure 17.** *In vivo* IHC analysis of TGF- β in the tissues around the non-grafted (A and C) and PMPC-grafted ePTFE (B and D) after 12 weeks. TGF-β was mainly detected near the edges of ePTFE fibers. The level of TGF-β expression

decreased between 4 and 12 weeks. At both time points, a 40–50% reduction in TGF- β expression was observed in the tissues around the PMPC-grafted ePTFE plates compared with that in the non-grafted plates. Images with a low magnification (A and B) and images with a high magnification (C and D) for the dotted rectangles in the A and B images. Quantitative analysis of TGF- β (+) cells in 36 areas (9 animals × 4 areas) of surrounding tissues (E) for each group after 4 and 12 weeks. Data are presented as mean ± S.E.M. (n = 36).

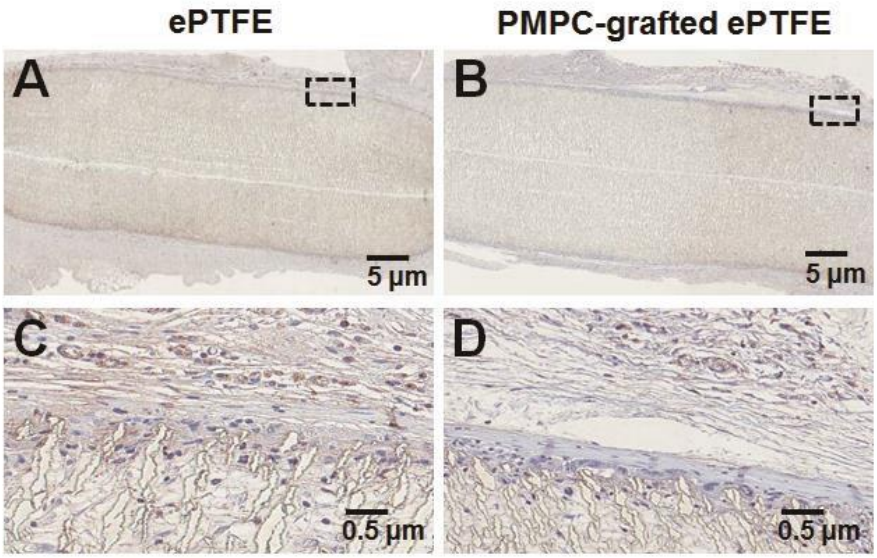


**Figure 18.** *In vivo* IHC analysis of MPO in the tissues around the nongrafted (A, C) and PMPC-grafted ePTFE (B, D) after 4 weeks. Images of a low magnification (A, B) and images with a high magnification (C, D) for the dotted rectangles in the A and B images. MPO expression was quite concentrated in the edge region and the expressed cells were much more identified in nongrafted plates than PMPC-grafted ePTFE plates after 4 weeks.

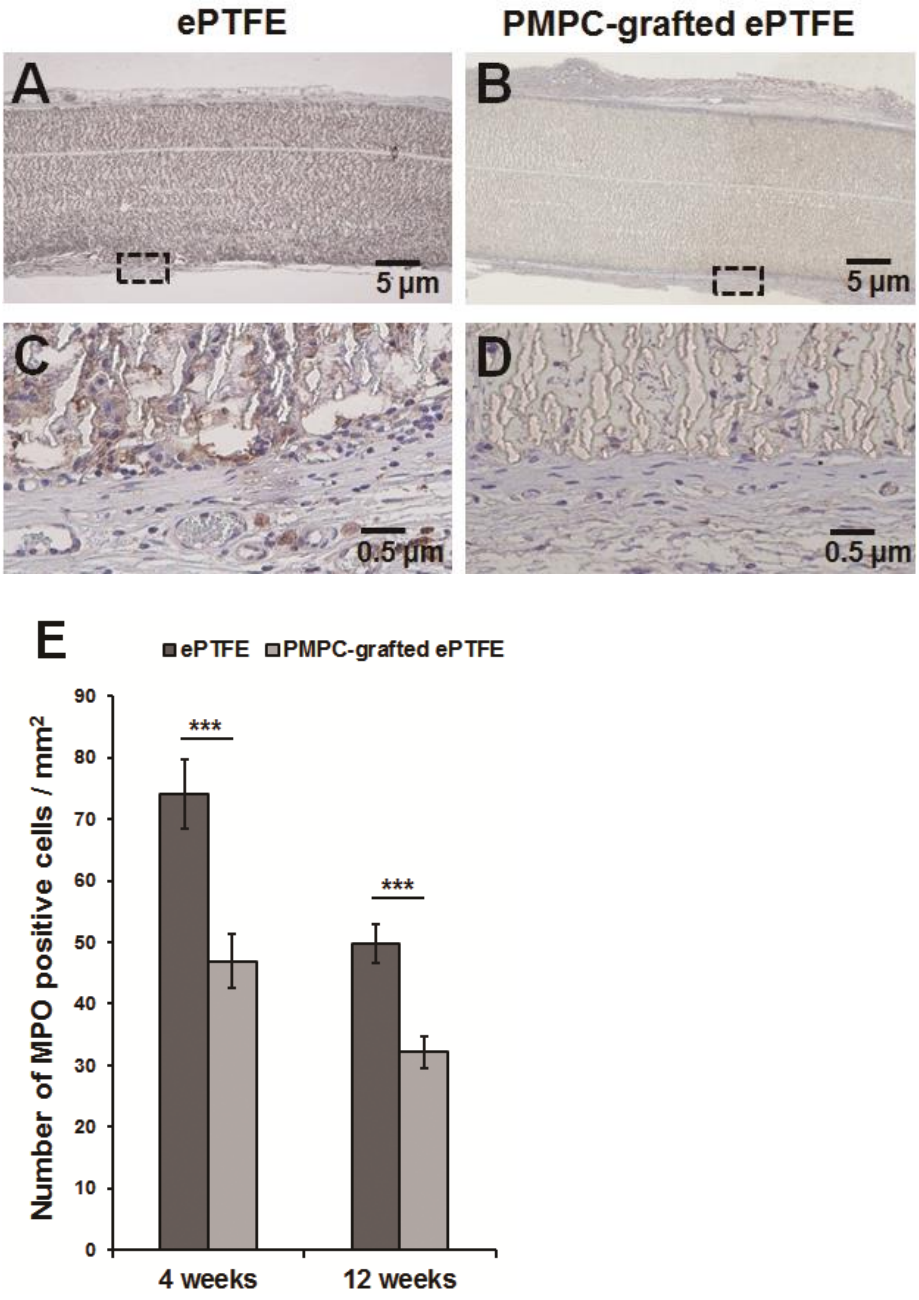


**Figure 19.** *In vivo* IHC analysis of MPO in the tissues around the non-grafted (A and C) and PMPC-grafted ePTFE (B and D) after 12 weeks. Number of

MPO positive cells was decreased between the two time points. The tissues around the PMPC-grafted ePTFE plates showed a reduction of approximately 40% in MPO expression compared with the tissues around the non-grafted plate. Images with a low magnification (A and B) and images with a high magnification (C and D) for the dotted rectangles in the A and B images. Quantitative analysis of MPO (+) cells in 36 areas (9 animals × 4 areas) of surrounding tissues (E) for each group after 4 and 12 weeks. Data are presented as mean ± S.E.M. (n = 36).

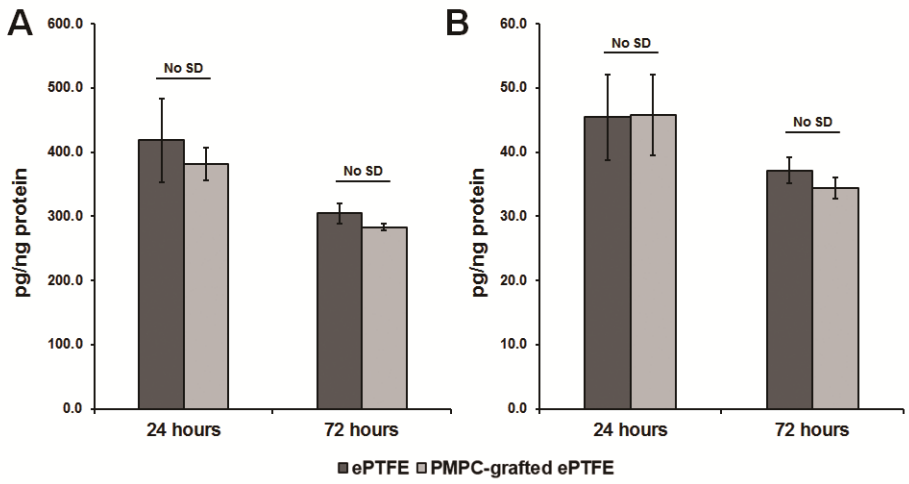


**Figure 20.** Acute inflammatory responses in the tissues around the non-grafted and PMPC-grafted ePTFE. Surrounding tissue samples were mechanically homogenized and analyzed by multiplex cytokine analysis kits. Quantitative analysis of (A) IL-6 and (B) TNF-α in surrounding tissues after 24 h and 72 h. There was no significant differences in both cytokines between non-grafted and PMPC-grafted ePTFE. Data are presented as mean ± S.E.M. (n = 8).

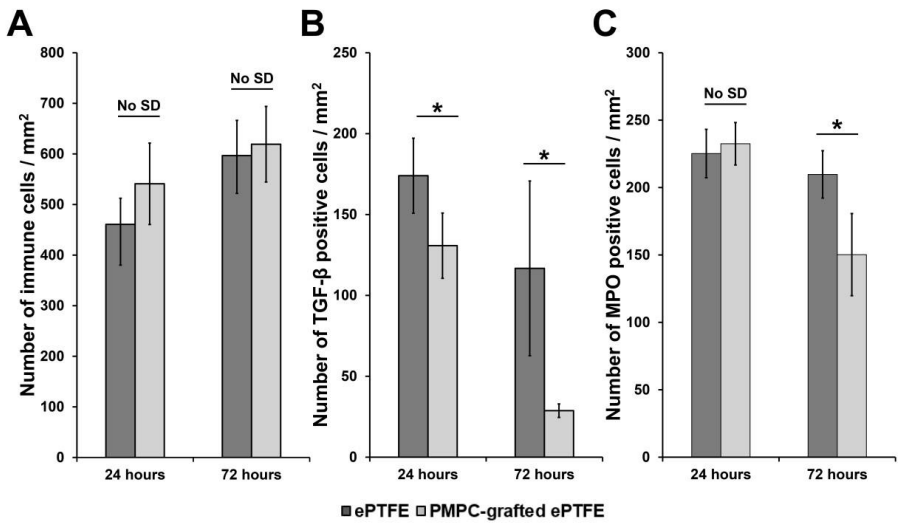


**Figure 21.** Quantitative analysis of immune cells (A), TGF-β cells (B) and MPO (C) in surrounding tissues after 24 and 72 h. Data are presented as mean ± SEM (n = 16). The number of inflammatory cells increased slightly between two time points. But the levels of TGF-β and MPO expression decreased during the period (A). A lower level of TGF-β expression was observed in the PMPC-grafted plate than in the non-grafted plate at both time points (B). A lower level of MPO in the tissues around the PMPC-grafted plate was only observed at 72 h (C).

| | C(%) | F(%) | O(%) | P(%) | N(%) | F(%)/C(%) |
|---|---|---|---|---|---|---|
| ePTFE | 31.89 | 64.86 | 3.25 | 0.00 | 0.00 | 2.03 |
| Reduced ePTFE | 40.97 | 57.06 | 1.96 | 0.00 | 0.00 | 1.39 |
| PMPC-grafted ePTFE | 54.50 | 26.37 | 15.67 | 2.12 | 1.34 | 0.48 |

**Table 1.** Atomic composition and F/C ratios quantified from the XPS spectra. Reduced ePTFE plate was prepared by reduction and UV irradiation of ePTFE in water without MPC monomers. P and N were estimated only in PMPC-grafted ePTFE surface, which supported the presence of phosphorylcholine moieties of PMPC polymers on the surface. The F/C ratio was decreased from 2.03 to 1.39 by the reduction process, supporting the defluorination reaction and the partial exchange of F to H. After successive PMPC polymerization following the reduction, the F/C ratio was further decreased to 0.48 and the content of N, P, and O was greatly increased, supporting that PMPC was successfully grafted on the ePTFE surface.

| Substrate | Young's Modulus (MPa) | Tensile strength (MPa) |
|---|---|---|
| Nongrafted ePTFE | 9.32 ± 0.75 | 6.50 ± 0.11 |
| PMPC-grafted ePTFE | 9.18 ± 0.72 | 7.06 ± 0.46 |

**Table 2.** Mechanical properties of nongrafted and PMPC-grafted ePTFE plates. Young's modulus and tensile strength are not significantly difference between non-grafted ePTFE and PMPC-grafted ePTFE.

# References


1. Gumpenberger T, Heitz J, Bäuerle D, Rosenmayer T. Modificati on of expanded polytetrafluoroethylene by UV irradiation in reac tive and inert atmosphere. Applied Physics A: Materials Science & Processing 2005; 80:27-33.
2. Ham J, Miller PJ. Expanded polytetrafluoroethylene implants in rhinoplasty: literature review, operative techniques, and outcome. Facial plastic surgery 2003; 19:331-340.
3. Kannan RY, Salacinski HJ, Butler PE, Hamilton G, Seifalian A M. Current status of prosthetic bypass grafts: a review. Journal of Biomedical Materials Research Part B: Applied Biomaterials 2005; 74:570-581.
4. Weiss MF, Scivittaro V, Anderson JM. Oxidative stress and incr eased expression of growth factors in lesions of failed hemodial ysis access. American journal of kidney diseases 2001; 37:970-9 80.
5. Ahlfeld SK, Larson RL, Collins HR. Anterior cruciate reconstruc tion in the chronically unstable knee using an expanded polytetr afluoroethylene (PTFE) prosthetic ligament. The American journa l of sports medicine 1987; 15:326-330.
6. Jin H-R, Lee J-Y, Yeon J-Y, Rhee C-S. A Multicenter evaluatio n of the safety of Gore-Tex as an implant in Asian rhinoplasty.

American Journal of Rhinology 2006; 20:615-619.

7. Venault A, Chang Y, Hsu H-Het al. Biofouling-resistance contro l of expanded poly(tetrafluoroethylene) membrane via atmospheri c plasma-induced surface PEGylation. Journal of Membrane Scie nce 2013; 439:48-57.

8. Sato Y, Murahara M. Protein adsorption on PTFE surface modif ied by ArF excimer laser treatment. Journal of Adhesion Scienc e and Technology 2004; 18:1545-1555.

9. Anderson JM, Rodriguez A, Chang DT. Foreign body reaction t o biomaterials. Seminars in immunology 2008; 20:86-100.

10. Hu W-J, Eaton JW, Ugarova TP, Tang L. Molecular basis of bi omaterial-mediated foreign body reactions. Blood 2001; 98:1231-1238.

11. Carpentier A, Latrémouille C, Cholley Bet al. First clinical use of a bioprosthetic total artificial heart: report of two cases. The Lancet 2015; 386:1556-1563.

12. Martin LG, MacDonald MJ, Kikeri D, Cotsonis GA, Harker LA, Lumsden AB. Prophylactic Angioplasty Reduces Thrombosis in Virgin ePTFE Arteriovenous Dialysis Grafts with Greater than 5 0% Stenosis: Subset Analysis of a Prospectively Randomized St udy. Journal of Vascular and Interventional Radiology 1999; 10: 389-396.

13. Raju S. PTFE grafts for hemodialysis access. Techniques for ins ertion and management of complications. Annals of surgery 198

7; 206:666.

14. Kang ET, Zhang Y. Surface modification of fluoropolymers via molecular design. Advanced Materials 2000; 12:1481-1494.

15. Yao K, Huang XD, Huang XJ, Xu ZK. Improvement of the sur face biocompatibility of silicone intraocular lens by the plasma-i nduced tethering of phospholipid moieties. Journal of biomedical materials research Part A 2006; 78:684-692.

16. Sin M-C, Chen S-H, Chang Y. Hemocompatibility of zwitterioni c interfaces and membranes. Polymer Journal 2014; 46:436-443.

17. Gong YK, Liu LP, Messersmith PB. Doubly biomimetic catecho lic phosphorylcholine copolymer: a platform strategy for fabricati ng antifouling surfaces. Macromolecular bioscience 2012; 12:979-985.

18. Jhong JF, Venault A, Hou CCet al. Surface zwitterionization of expanded poly(tetrafluoroethylene) membranes via atmospheric pl asma-induced polymerization for enhanced skin wound healing. ACS applied materials & interfaces 2013; 5:6732-6742.

19. Goda T, Konno T, Takai M, Moro T, Ishihara K. Biomimetic p hosphorylcholine polymer grafting from polydimethylsiloxane surf ace using photo-induced polymerization. Biomaterials 2006; 27:5 151-5160.

20. Lewis A, Tolhurst L, Stratford P. Analysis of a phosphorylcholi ne-based polymer coating on a coronary stent pre-and post-impla ntation. Biomaterials 2002; 23:1697-1706.

21. Whelan D, Van der Giessen W, Krabbendam Set al. Biocompatibility of phosphorylcholine coated stents in normal porcine coronary arteries. Heart 2000; 83:338-345.

22. Ishihara K. Bioinspired phospholipid polymer biomaterials for making high performance artificial organs. Science and Technology of Advanced Materials 2000; 1:131-138.

23. Moro T, Takatori Y, Ishihara Ket al. Surface grafting of artificial joints with a biocompatible polymer for preventing periprosthetic osteolysis. Nature materials 2004; 3:829-836.

24. Park JU, Ham J, Kim Set al. Alleviation of capsular formations on silicone implants in rats using biomembrane-mimicking coatings. Acta biomaterialia 2014; 10:4217-4225.

25. Kang S, Lee M, Kang Met al. Development of anti-biofouling interface on hydroxyapatite surface by coating zwitterionic MPC polymer containing calcium-binding moieties to prevent oral bacterial adhesion. Acta biomaterialia 2016; 40:70-77.

26. Kakinoki S, Sakai Y, Takemura Tet al. Gene chip/PCR-array analysis of tissue response to 2-methacryloyloxyethyl phosphorylcholine (MPC) polymer surfaces in a mouse subcutaneous transplantation system. Journal of biomaterials science Polymer edition 2014; 25:1658-1672.

27. Le QT, Naumov S, Conard Tet al. Mechanism of modification of fluorocarbon polymer by ultraviolet irradiation in oxygen atmosphere. ECS Journal of Solid State Science and Technology 20

13; 2:N93-N98.

28. Ostuni E, Chapman RG, Liang MNet al. Self-assembled monola yers that resist the adsorption of proteins and the adhesion of b acterial and mammalian cells. Langmuir : the ACS journal of su rfaces and colloids 2001; 17:6336-6343.

29. Saidi IS, Biedlingmaier JF, Whelan P. In vivo resistance to bact erial biofilm formation on tympanostomy tubes as a function of tube material. Otolaryngology--Head and Neck Surgery 1999; 12 0:621-627.

30. Noh I, Chittur K, Goodman SL, Hubbell JA. Surface modificati on of poly (tetrafluoroethylene) with benzophenone and sodium hydride by ultraviolet irradiation. Journal of Polymer Science Pa rt A: Polymer Chemistry 1997; 35:1499-1514.

31. Mihály J, Sterkel S, Ortner HMet al. FTIR and FT-Raman spect roscopic study on polymer based high pressure digestion vessels. Croatica chemica acta 2006; 79:497-501.

32. Noh I, Hubbell JA. Photograft polymerization of acrylate mono mers and macromonomers on photochemically reduced PTFE fil ms. Journal of Polymer Science Part A: Polymer Chemistry 199 7; 35:3467-3482.

33. Ito Y, Ochiai Y, Park YS, Imanishi Y. pH-sensitive gating by c onformational change of a polypeptide brush grafted onto a poro us polymer membrane. Journal of the American Chemical Societ y 1997; 119:1619-1623.

34. Kojima M, Ishihara K, Watanabe A, Nakabayashi N. Interaction between phospholipids and biocompatible polymers containing a phosphorylcholine moiety. Biomaterials 1991; 12:121-124.

35. Schlenoff JB. Zwitteration: coating surfaces with zwitterionic fun ctionality to reduce nonspecific adsorption. Langmuir : the ACS journal of surfaces and colloids 2014; 30:9625-9636.

36. Seetho K, Zhang S, Pollack KAet al. Facile Synthesis of a Pho sphorylcholine-Based Zwitterionic Amphiphilic Copolymer for An ti-Biofouling Coatings. ACS Macro Letters 2015; 4:505-510.

37. Inanli S, Sari M, Baylancicek S. The use of expanded polytetraf luoroethylene (Gore-Tex) in rhinoplasty. Aesthetic plastic surgery 2007; 31:345-348.

38. Maas CS, Gnepp DR, Bumpous J. Expanded polytetrafluoroethyl ene (Gore-Tex soft-tissue patch) in facial augmentation. Archives of Otolaryngology–Head & Neck Surgery 1993; 119:1008-1014.

39. Godin MS, Waldman SR, Johnson CM. The use of expanded p olytetrafluoroethylene (Gore-Tex) in rhinoplasty: a 6-year experie nce. Archives of Otolaryngology–Head & Neck Surgery 1995; 1 21:1131-1136.

40. Catanese J, Cooke D, Maas C, Pruitt L. Mechanical properties o f medical grade expanded polytetrafluoroethylene: the effects of internodal distance, density, and displacement rate. Journal of Bi omedical Materials Research Part A 1999; 48:187-192.

41. Franz S, Rammelt S, Scharnweber D, Simon JC. Immune respon

ses to implants - a review of the implications for the design of immunomodulatory biomaterials. Biomaterials 2011; 32:6692-6709
.

42. Ratner BD. Reducing capsular thickness and enhancing angiogen esis around implant drug release systems. Journal of Controlled Release 2002; 78:211-218.

43. Liu P-S, Chen Q, Wu S-S, Shen J, Lin S-C. Surface modificati on of cellulose membranes with zwitterionic polymers for resista nce to protein adsorption and platelet adhesion. Journal of Mem brane Science 2010; 350:387-394.

44. Ishihara K, Tsuji T, Kurosaki T, Nakabayashi N. Hemocompatib ility on graft copolymers composed of poly (2-methacryloyloxyet hyl phosphorylcholine) side chain and poly (n-butyl methacrylate ) backbone. Journal of biomedical materials research 1994; 28:2 25-232.

45. Zhang Q, Wang C, Babukutty Y, Ohyama T, Kogoma M, Koda ma M. Biocompatibility evaluation of ePTFE membrane modifie d with PEG in atmospheric pressure glow discharge. Journal of biomedical materials research 2002; 60:502-509.

46. Wang Y, Tang Z, Xue Ret al. TGF-β1 promoted MMP-2 media ted wound healing of anterior cruciate ligament fibroblasts throu gh NF-κB. Connective tissue research 2011; 52:218-225.

47. Broughton G, 2nd, Janis JE, Attinger CE. The basic science of wound healing. Plastic and reconstructive surgery 2006; 117:12S-

34S.

48. Kolb CM, Pierce LM, Roofe SB. Biocompatibility comparison o f novel soft tissue implants vs commonly used biomaterials in a pig model. Otolaryngology--head and neck surgery : official jo urnal of American Academy of Otolaryngology-Head and Neck Surgery 2012; 147:456-461.

49. Letterio JJ, Roberts AB. Regulation of immune responses by TG F-β. Annual review of immunology 1998; 16:137-161.

50. Klebanoff SJ, Kettle AJ, Rosen H, Winterbourn CC, Nauseef W M. Myeloperoxidase: a front-line defender against phagocytosed microorganisms. Journal of leukocyte biology 2013; 93:185-198.

51. Cassady AI, Hidzir NM, Grøndahl L. Enhancing expanded poly (tetrafluoroethylene)(ePTFE) for biomaterials applications. Journal of Applied Polymer Science 2014; 131.

52. Ye SH, Johnson CA, Jr., Woolley JRet al. Simple surface modif ication of a titanium alloy with silanated zwitterionic phosphoryl choline or sulfobetaine modifiers to reduce thrombogenicity. Colloids and surfaces B, Biointerfaces 2010; 79:357-364.

# 국문초록

서론 : 고어텍스로 더 잘 알려진 ePTFE는 조작하기 쉬운 기계적 성질과 생화학적 안정성 때문에, 이식 가능한 생체 재료로 널리 사용 되고 있다. 그러나 급성 혹은 만성적으로 지속되는 감염 및 염증 반응은 ePTFE 이식 후 주요 부작용으로 보고 되었다. 이와 같은 부작용을 최소화하기 위해서 ePTFE 표면에 항염 작용이 있는것으로 알려진, 생체막 모방 중합체인 PMPC를, 공유결합을 이용해 코팅 하였다. 본 연구는, PMPC 코팅 으로 인한 ePTFE의 항염, 항균 작용 상승 효과에 대해 실험적으로 평가해 보고자 한다.

재료 및 방법 : Water contact angle, XPS, 전자 현미경 사진 등을 측정하여 코팅으로 인한 ePTFE의 표면 변화에 대해 평가 하였으며, 코팅된 고어텍스 자체의 항염, 항균 작용에 대한 평가를 위해 단백질 흡착, 섬유 아세포 및 세균 부착 실험을 시행하였다. 34마리의 수컷 Sprague-Dawley rat의 양측 등에 각각 코팅한

고어텍스 판과 코팅하지 않는 고어텍스 판을 이식하였으며, 이식 수술 후 24시간, 72시간, 4주, 12주에 채취하여 염증세포 및 염증인자의 변화에 대해 분석하였다.

결과 : PMPC 코팅은 ePTFE 표면에 단백질 흡착과 섬유 아세포 부착을 모두 감소시켰다. 또한 ePTFE 인체 이식 후 발생하는 염증 반응에서 가장 주요한 역할을 하는 균인 Staphylococcus aureus의 부착과 성장도 PMPC 코팅한 ePTFE군 에서 매우 유의미 하게 감소함을 알수 있었다. 동물 실험을 통해 염증 몇 면역 관련 인자 특히, transforming growth factor-β (TGF-β), myeloperoxidase (MPO)을 분석하였으며, 코팅하지 않는 군에 비하여 코팅한 군에서 유의미하게 염증세포의 수가 감소함을 증명 하였다.

결론 : PMPC 코팅은 ePTFE 이식으로 유발될 수 있는 염증 반응을 줄이는데 매우 효과적인 방법이다. 특히 공유결합을 이용한 PMPC 코팅은 ePTFE 이식의 항염 항균 작용을 상승시키는데 매우 효과적이어서, ePTFE의 의학적 적용시 부작용을 줄일 수 있는 유용한 방

법이다.

주요어 : 고어텍스, ePTFE, 생체막 모방 중합체, PMPC, 코팅

**학번 : 2014-30921**